Molybdenum and iron mutually impact their homeostasis in cucumber (Cucumis sativus) plants

rmed the presence of traits previously shown to confer drought resistance to plants, such as the synthesis of nitric oxide and of organic volatile organic compounds. We used the two strains on pepper (*Capsicuum annuum* L.) because of its

Summary

- Molybdenum (Mo) and iron (Fe) are essential micronutrients required for crucial enzyme activities in plant metabolism. Here we investigated the existence of a mutual control of Mo and Fe homeostasis in cucumber (*Cucumis sativus*).
- Plants were grown under single or combined Mo and Fe starvation. Physiological parameters were measured, the ionomes of tissues and the ionomes and proteomes of root mitochondria were profiled, and the activities of molybdo-enzymes and the synthesis of molybdenum cofactor (Moco) were evaluated.
- Fe and Mo were found to affect each other's total uptake and distribution within tissues and at the mitochondrial level, with Fe nutritional status dominating over Mo homeostasis and affecting Mo availability for molybdo-enzymes in the form of Moco. Fe starvation triggered Moco biosynthesis and affected the molybdo-enzymes, with its main impact on nitrate reductase and xanthine dehydrogenase, both being involved in nitrogen assimilation and mobilization, and on the mitochondrial amidoxime reducing component.
- These results, together with the identification of > 100 proteins differentially expressed in root mitochondria, highlight the central role of mitochondria in the coordination of Fe and Mo homeostasis and allow us to propose the first model of the molecular interactions connecting Mo and Fe homeostasis.

Introduction

Iron (Fe) is an essential micronutrient for plants and its uptake from soil and transport to all plant tissues together with the regulation of its homeostasis during various biotic/abiotic stresses have been studied (Jeong & Guerinot, 2009; Ivanov *et al*., 2012; Kobayashi & Nishizawa, 2012; Ravet & Pilon, 2013; Briat *et al*., 2015a). The negative agronomic and economic impact of plant Fe nutritional deficiency, most frequently occurring in calcareous soils, led to a variety of experimental approaches aimed at elucidating Fe homeostasis in plant organs and organelles (Palmer & Guerinot, 2009). Among these approaches, -omics technologies were applied to tissues from several plant species grown under Fe deficiency. Transcriptomics revealed the complex set of genes involved in the Fe deficiency response and identified the master regulators of such a response (Colangelo & Guerinot, 2004; Lingam *et al*., 2011; Meiser *et al*., 2011), together with those supporting the metabolic changes occurring under Fe deficiency (Rellán-Álvarez *et al*., 2011; Schuler *et al*., 2011; Ciaffi *et al*., 2013; Rodriguez-Celma *et al*., 2013; Li *et al*., 2014; Moran Lauter *et al*., 2014; Paolacci *et al*., 2014). Proteomics and metabolomics clarified the impact of Fe on carbon, nitrogen and sulphur metabolism, on the production of secondary metabolites and on the production of enzymes counteracting oxidative stress (Li *et al*., 2008; Donnini *et al*., 2010; Lan *et al*., 2011; Lopez-Millan *et al*., 2013; Sudre *et al*., 2013; Lima *et al*., 2014; Schmidt *et al*., 2014).

Nonetheless, many aspects of subcellular Fe homeostasis are still poorly understood (Vigani *et al*., 2013a,c). While changes in the protein profile occurring in thylakoids from Fe-deficient plants have been analysed in detail (Andalus *et al*., 2006; Timperio *et al*., 2007; Laganowsky *et al*., 2009;

Lopez-Millan *et al*., 2013), element, protein and metabolite profiling of mitochondria from plants grown under Fe starvation have still not been documented.

Ionomics revealed that changes in the Fe nutritional status of a plant are associated with changes in a given subset of elements, including molybdenum (Mo) (Baxter *et al*., 2008a; Baxter, 2009; Murgia & Vigani, 2015). The transition metal Mo is an essential micronutrient (in traces), taken up in the form of molybdate, for nearly all organisms including plants (Bittner & Mendel, 2010; Shinmachi *et al*., 2010; Llamas *et al*., 2011; Bittner, 2014). In higher plants, a few molybdate transporters have been identified belonging to the family of sulphate transporters, namely molybdate transporter (MOT1) (Tomatsu *et al*., 2007; Baxter *et al*., 2008b; Ide *et al*., 2011) and MOT2 (Gasber *et al*., 2011) in Arabidopsis, and sulfate transporter in *Stylosanthes hamata* (Fitzpatrick *et al*., 2008). MOT1 is localized either in mitochondria or in endomembranes, as reported by Baxter *et al*. (2008b) and Tomatsu *et al*. (2007), respectively, whereas MOT2 exports the stored molybdate from vacuoles to provide it to maturing seeds in senescing plants (Gasber *et al*., 2011). Molybdate itself is biologically inactive and needs to be complexed by a Mo-binding pterin to form the biologically functional Mo cofactor (Moco). Moco biosynthesis starts in the mitochondrion, with circularization of GTP by Cnx2 and Cnx3 (cyclic pyranopterin monophosphate synthase) enzymes to produce cyclic pyranopterin monophosphate (cPMP). The cPMP intermediate is then exported out of the mitochondrion into the cytosol, where the biosynthesis of Moco is completed in three steps (Bittner & Mendel, 2010). Moco is inserted into the molybdo-enzymes nitrate reductase (NR), sulphite oxidase (SO), xanthine dehydrogenase (XDH) and aldehyde oxidase (AO) which have key roles in either essential or important metabolic processes such as nitrogen assimilation, detoxification of sulphite, purine catabolism and synthesis of abscisic acid (ABA), respectively. A fifth group of molybdo-enzymes, whose members are homologues of the human molybdo-enzyme mitochondrial amidoxime reducing component (mARC), which catalyses the reduction of a variety of *N*-hydroxylated substrates, exists in the genomes of algae, monocots and dicots (Ott *et al*., 2015). Nearly all eukaryotic genomes with Mo metabolism encode two mARC proteins and all mammalian mARC proteins are characterized by the presence of an N-terminal extension, which targets the mARC protein either to the outer (e.g. pig) or the inner (e.g. mouse) mitochondrial membrane (Ott *et al*., 2015). In Arabidopsis, mARC-2 carries a mitochondrial presequence whereas mARC-1 is lacking such an N-terminal extension, suggesting that these proteins are differentially localized.

The ARC protein from the green alga *Chlamydomonas reinhardti* is capable of eliminating *N*-hydroxylated and thus mutagenic base analogues (Chamizo-Ampudia *et al*., 2011), whereas the Arabidopsis mARC-1 can generate nitric oxide during nitrite reduction (Yang *et al*., 2015). However, the *in vivo* physiological roles and the subcellular localization of plant ARC proteins are still unknown.

In addition, a Moco carrier protein (MCP), whose physiological function is likewise not fully understood but which is proposed to distribute Moco to the various molybdo-enzymes, has been identified in green algae (Witte *et al*., 1998) and functional homologues may also exist in higher plants.

The existence of an interaction between Mo and Fe metabolisms is supported by evidence in the literature (Bittner, 2014). The following observations support an interaction between Mo and Fe: several genes of Mo metabolism are regulated by Fe availability; most molybdo-enzymes also require Fe-containing redox groups, such as Fe-S clusters (XDH and AO) or haem (NR and human SO); Moco biosynthesis and the cytosolic Fe-S cluster assembly (CIA) machinery utilize the same mitochondrial ABC transporter ATM3, belonging to the ATP-binding cassette B superfamily

(ABCB) (Balk & Schaedler, 2014). This ATM3 transporter is involved in the export of the Moco intermediate cPMP from mitochondria to the cytosol (Teschner *et al*., 2010), as well as in the transport of glutathione polysulphide for Fe-S cluster assembly (Schaedler *et al*., 2014).

While the co-evolution of Mo and Fe in metabolism and in enzymes has been noted in general (Anbar, 2008; Bittner, 2014; Yokoyama & Leimkühler, 2015), no experiments have yet been undertaken to unravel the physiological relationship between Mo and Fe with respect to uptake, storage, distribution and consumption by enzymes and organelles. Thus, the goal of the present work was to begin to fill this gap in our knowledge.

We investigated the early physiological, ionomic and biochemical changes occurring in cucumber (*Cucumis sativus*) roots and leaves under single or combined Mo and Fe starvation. Roots are responsible for nutrient uptake from soil and their mitochondria play a central role in the metabolic reprogramming occurring in Fe-deficient roots (Vigani, 2012; Vigani *et al*., 2016). Moreover, mitochondria synthesize both Fe-S clusters (Balk & Schaedler, 2014) and the first intermediate in Moco biosynthesis (Teschner *et al*., 2010). We also obtained a detailed close-up of root mitochondria and we profiled their ionomes and proteomes.

Our results provide the first experimental proof of a reciprocal impact of Mo and Fe homeostasis and we propose a novel model for such crosstalk.

Materials and Methods

Plant growth

Cucumber (*Cucumis sativus* L. cv Marketmore) seeds were sown in Agriperlite (Agrilit; Perlite Italiana srl, Corsico, MI, Italy), watered with 0.1 mM $CaSO_4$, allowed to germinate in the dark at 26°C for 3 d, then transferred to a nutrient solution and grown as reported in Vigani *et al*. (2013b); control medium is indicated as +Mo+Fe. Fe(III)-EDTA and/or $(NH_4)Mo_7O_{24}$ was omitted in −Fe and/or −Mo medium, respectively.

Physiological parameters

Segments of leaves (*c*. 2 cm × 2 cm) were cut and weighed, and oxygen evolution and consumption were measured at 200 or 800 μE m^{-2} s^{-1} according to Tarantino *et al*. (2010) and tissue was then put in vials containing 2–6 ml of dimethyl formamide for chlorophyll extraction and quantification, according to Tarantino *et al*. (2005). Rates were analysed with OXYLAB v.1.15 software (Hansatech Instruments Ltd, Norfolk, UK).

Purification of root mitochondria

Mitochondria were isolated according to Vigani *et al*. (2009). To test the purity of the mitochondrial fractions, the samples were loaded on a discontinuous sodium dodecyl sulphate (SDS)-polyacrylamide gel according to Vigani *et al*. (2016) and three different antibodies were used: a monoclonal antibody against maize (*Zeas mays*) porin (Balk & Leaver, 2001), a polyclonal antibody against Arabidopsis translocase of the chloroplast envelope (Toc33) (Rödiger *et al*., 2010) and a polyclonal antibody against *Cucurbita* sp. Amakuri Nankin catalase (Yamaguchi & Nishimura, 1984).

Ionomics

Leaves of cucumber plants (cut at the petiole) and their roots were thoroughly rinsed in distilled water; water was gently removed with absorbent paper and samples were placed in calibrated 15-ml tubes (five leaves per tube). Mitochondrial fractions were obtained according to Vigani *et al*. (2009) with a few modifications. To minimize peroxisomal contaminations, the fractions were loaded on a percoll gradient and, after centrifugation at 40 000 ***g*** for 45 min, mitochondria were removed from the 28%/40% interface, while the peroxisomal fraction was removed from the bottom of the tube, according to Millar *et al*. (2007). The concentrations of various elements were then measured by inductively coupled plasma−mass spectrometry (ICP-MS), according to Vigani *et al*. (2013b). Statistical analysis was performed using Duncan's test with SPSS software (SPSS Statistics, IBM, Armonk, NY, USA).

Chemical detection of Moco, MPT and cPMP

Moco and its metal-free precursors MPT and cPMP were detected according to Teschner *et al*. (2010), with the following volume adjustments: oxidation was performed with 200 mg of root or leaf material, in 400 µl of 0.1 M Tris-HCl, pH 7.2, and by addition of 150 µl of acidic iodine; excess iodine was reduced by the addition of 112 µl of 1% ascorbic acid. Relative amounts of FormA-dephospho (the common oxidation derivative of Moco and MPT) and CompoundZ (the oxidation derivative of cPMP) are given as relative peak areas per mg of protein. FormA-dephospho hence represents the sum of Moco and of its ultimate Mo-free precursor MPT, as the applied method is incapable of differentiating between these two molecules.

Assays of molybdo-enzyme activities

XDH, AO, NR and SO activities were measured according to Teschner *et al*. (2010). For XDH and AO activities, the relative densities of the resulting activity bands were determined by using IMAGEJ software version 1.38 from NIH (http://rsb.info.nih.gov/ij).

Sample preparation for proteomic analysis

Mitochondrial fractions were resuspended in resuspension buffer (Vigani *et al*., 2009) and centrifuged twice at 12 000 ***g*** for 20 min. Rapigest 0.2% (Waters Corporation, Milford, MA, USA) was added and the mixture was heated at 100°C for 20 min. It was then centrifuged at 2200 ***g*** for 10 min and the supernatant was digested with 1.5 µg of trypsin (Sequencing Grade Modifier Trypsin, Promega) overnight at 37°C. The reaction was stopped by acidification with 0.5% trifluoroacetic acid and the mixture was incubated for 45 min at 37°C. After centrifugation at 13 000 ***g*** for 10 min, the resulting peptide mixture was desalted with PepClean C-18 spin columns (Pierce Biotechnology, Rockford, IL, USA) and resuspended in 0.1% formic acid.

Western blot analysis

Purified mitochondria were fractionated into mitochondrial soluble fraction (MSF) and integral mitochondrial membrane fraction (MMF) according to Tan *et al*. (2010) with a few modifications. Intact isolated mitochondria were suspended in milliQ water (Merck-Millipore, Darmstadt, Germany) before lysis by six freeze/thaw cycles and the soluble proteins were collected in the supernatant following centrifugation at 20 000 ***g***. Organic material was then heated at 160°C for 5 h in nitric acid. The acid digest was diluted to < 2% (v/v) HNO_3 and passed through 0.22-mm filters (Millipore). Fe and Mo contents were quantified using ICP-MS technology. The separation between

MMF and MSF was tested by measuring the activity of citrate syntase (CS; a matrix-soluble enzyme), according to Vigani *et al*. (2009). In control mitochondrial fractions, CS activity was 420, 550 and 18 nmol thionitrobenzoic acid (TNB) mg protein^{-1} in intact mitochondria, MSF and MMF, respectively. Six micrograms of MMF was electrophoresed on 12% SDS-polyacrylamide gels, blotted onto a polyvinylidene difluoride membrane and immunodecorated with polyclonal antibodies against the marker protein cytochrome c oxidase subunit II (COX II) (purchased from Agrisera AB, Vännäs, Sweden) and with polyclonal antibodies raised against recombinant pmARC-1 and pmARC-2 proteins from Arabidopsis, with the mARC-2 protein lacking the putative N-terminal mitochondrial targeting sequence. Expression in *Escherichia coli* and purification of these proteins were performed as previously described for human mARCs (Gruenewald *et al*., 2008; Kotthaus *et al*., 2011). Antibodies were diluted 1 : 1000 in TBST buffer (tris-buffered saline-Tween 20) containing 5% milk powder. An alkaline phosphatase-conjugated anti-rabbit immunoglobulin G (IgG) was used (Promega; 1 : 10 000 dilution in TBST buffer containing 5% milk powder) in combination with the 5-bromo-4-chloro-3′-indolyphosphate p-toluidine salt/nitro-blue tetrazolium chloride (BCIP/NBT) staining system (Fisher Scientific, Schwerte, Germany).

Multidimensional Protein Identification Technology (MudPIT) analysis and tandem mass spectra (MS/MS) data processing

Peptide mixtures were analysed using MudPIT (Delahunty & Yates, 2007) (further details are reported in Methods S1).

The experimental tandem mass spectra were matched against the cucumber protein sequences retrieved from the National Center for Biotechnology Information (NCBI) database (http://www.ncbi.nlm.nih.gov) released in January 2014. Data processing was performed using BIOWORKS 3.3.1 software (ThermoFisher Scientific, San Josè, CA, USA), based on the SEQUEST algorithm (Ducret *et al*., 1998). 'No enzyme' mode and a mass tolerance of 0.5 amu for precursor ions were used. Peptide and protein assignments were made according to specific guidelines (Carr *et al*., 2004); X correlation was set to 2.0 for +1, 2.5 for +2 and 3.5 for +3 charge states, respectively. The maximum value for peptide/protein probability was set to 10^{-3}, while the minimum value for the SEQUEST-based SCORE was set to 10. Finally, the false discovery rate (FDR) was determined using a decoy database (Wang *et al*., 2009) for cucumber; FDR resulted < 3%.

Proteomics data-mining and label-free quantification

The spectral count (SpC) values of the identified proteins were normalized using a total signal normalization method (Carvalho *et al*., 2008) and compared using a label-free quantification approach (Mauri *et al*., 2005; Regonesi *et al*., 2006). The considered protein lists (+Mo+Fe, n = 6; −Mo+Fe, n = 6; +Mo−Fe, n = 8; −Mo−Fe, n = 7) were first processed by linear discriminant analysis (LDA) (Hilario & Kalousis, 2008), applying a common covariance matrix for all groups and the Mahalanobis distance (Jain *et al*., 1999). To discriminate the analysed plant conditions, proteins with the largest (≥ 3) and smallest F ratio and P-value (≤ 0.05) were selected. The average spectral count (aSpC) value of the proteins selected by LDA was further processed using the Differential Average (DAve) index (Mauri & Dehò, 2008). In the considered comparisons (+Mo+Fe vs −Mo+Fe; +Mo+Fe vs +Mo−Fe; +Mo+Fe vs −Mo−Fe), the best DAve value or those >|0.2| were retained for each protein (Supporting Information Methods S1). The DAve index was calculated as (aSpC_C – aSpC_D)/(aSpC_C + aSpC_D)/0.5, where aSpC_C and aSpC_D are the aSpC value of a given protein in the control condition C and in a given deficiency condition D,

respectively. Fold change was estimated using the natural logarithm of the spectral count ratio aSpC_C/aSpC_D. Conventionally, the DAve value of proteins identified exclusively in one of the two compared conditions was set to ± 2, while the natural logarithm of the spectral count ratio of the same protein was set to ± 100. Proteins selected by LDA and MAProMA (Multidimensional Algorithm Protein Map) were processed by hierarchical clustering (Zhao & Karypis, 2005) applying Ward's method and a Euclidean distance metric.

Results

Fe starvation induces increased Mo uptake and its accumulation in roots

Cucumber plants were grown under single or combined Mo and Fe starvation in a 22-d time-course experiment to identify the most suitable sampling day for obtaining a broad picture of the specific responses triggered by the applied nutritional deficiencies, before the onset of general stress responses.

Plants were collected after 10 (Fig. 1), 15 (Fig. S1) and 22 d (Fig. S2) and physiological parameters were measured: fresh weight (FW), chlorophyll content, and O_2 evolution and consumption were all impaired by Fe starvation (Fig. S3). A reduction of FW and an increase in chlorophyll content and O_2 evolution occurred under Mo starvation at 22 d. Such an increase in O_2 evolution can be attributed to the higher chlorophyll content in leaves of Mo-deficient plants (−Mo), as no differences emerged if O_2 evolution was calculated with respect to chlorophyll content (as μmol O_2 min^{-1} mg^{-1} chlorophyll).

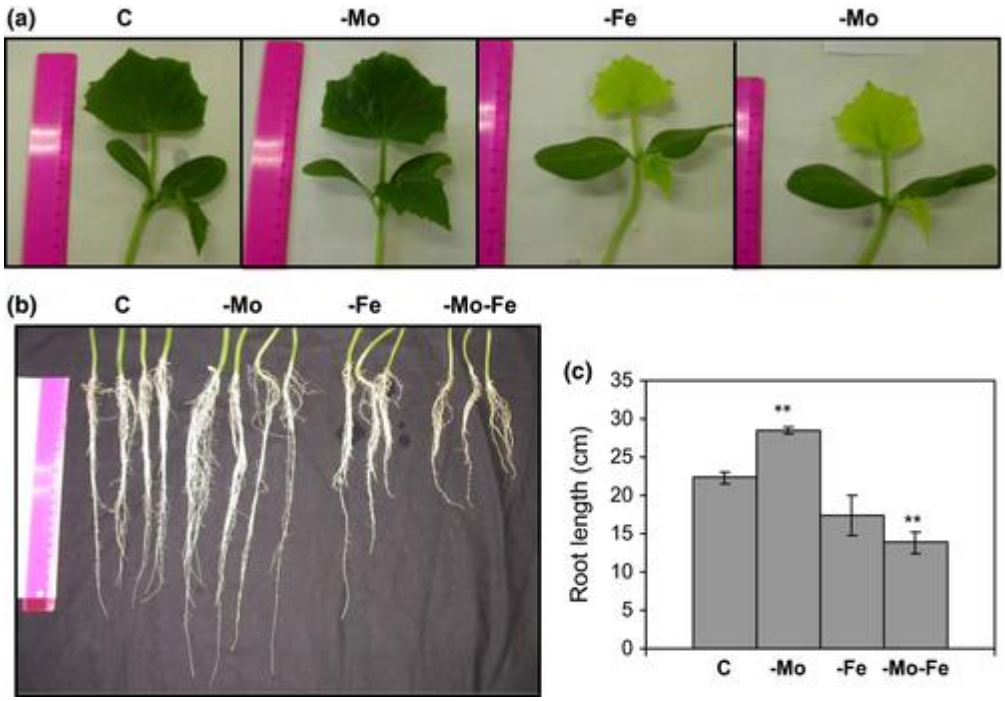

Figure 1

Open in figure viewerPowerPoint

Cucumber plants grown under single or combined molybdenum (Mo) and iron (Fe) starvation. (a) Symptoms of plants grown for 10 d in control (C) hydroponic medium (+Mo+Fe), and in medium

devoid of Mo (−Mo), devoid of Fe (−Fe), or devoid of both micronutrients (−Mo−Fe). (b) Ten-day-old roots from plants described in (a). (c) Root lengths from plants described in (a) (in cm). Bars represent mean values ± SE of at least three independent samples. Significant differences with respect to control: **, $P < 0.01$, according to Student's *t*-test.

Caption

Most of these parameters were unaffected by isolated Mo starvation at the earliest investigated time-point. Nevertheless, plants of that age were already responding to isolated or combined deficiencies, as roots of Mo-deficient plants were longer than roots of control plants (Fig. 1b,c), whereas roots of −Mo−Fe plants presented impaired growth (Fig. 1b,c). For all further experiments described below, tissues (roots and leaves) were thus sampled from 10-d-old plants. Analysis of the Fe deficiency-induced response in 10-d-old cucumber plants has already been described (Vigani *et al*., 2009, 2016; Vigani & Zocchi, 2010) and it allows the collection of sufficient plant biomass for further analysis.

The ionomes of plants were profiled by quantifying the contents of macronutrients and micronutrients in both roots (Fig. 2a) and leaves (Fig. 2b).

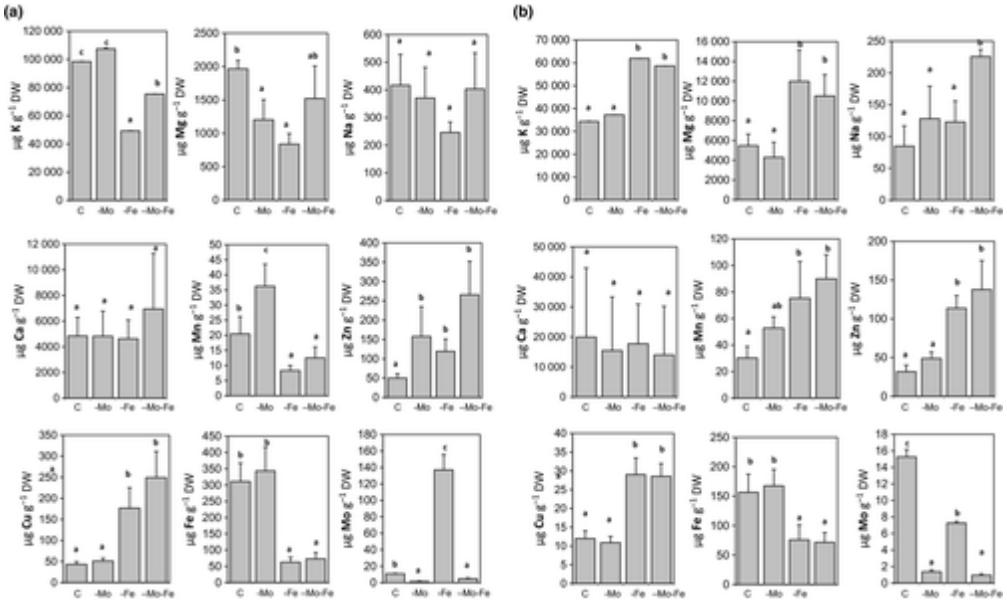

Figure 2

Open in figure viewerPowerPoint

Leaf and root ionomes of cucumber plants grown under single or combined molybdenum (Mo) and iron (Fe) starvation. (a) Root ionomes from plants grown for 10 d in control (C) hydroponic medium (+Mo+Fe), and in medium devoid of Mo (−Mo), devoid of Fe (−Fe), or devoid of both micronutrients (−Mo−Fe). (b) Leaf ionomes from plants grown as in (a). Bars represent mean values ± SE of four independent samples. Different letters indicate statistically significant difference ($P < 0.05$).

Caption

Molybdenum and Fe starvation affected Mo and Fe contents in roots, as demonstrated by a reduced Fe content in Fe-starved roots and a reduced Mo content in Mo-starved roots. Mo concentrations increased > 10-fold in response to Fe starvation in roots (Fig. 2a).

In the same tissue, potassium (K) concentrations decreased upon Fe starvation, with this decrease being attenuated by additional Mo starvation. Magnesium (Mg) concentrations decreased in both isolated deficiencies, while combined Mo and Fe starvation had a less severe impact on Mg

concentrations, as seen for K concentrations. Other than K and Mg, zinc (Zn) concentrations increased in both isolated and combined Mo and Fe deficiencies. Mo starvation caused accumulation of manganese (Mn), whereas Fe and combined Mo/Fe starvation resulted in severely reduced Mn concentrations. Copper (Cu) concentrations are clearly dependent on Fe but not on Mo availability, as Cu concentrations were unaltered in Mo-starved roots whereas they increased to about the same extent in Fe- and Mo/Fe-starved roots. Lastly, no significant alterations in sodium (Na) and calcium (Ca) contents were observed in roots (Fig. 2a).

Growth of plants under Mo and Fe starvation also affected Mo and Fe contents in leaves, with Fe contents being strongly reduced in Fe-starved leaves and Mo contents being even more reduced in Mo-starved leaves (Fig. 2b). In addition, Mo concentrations decreased in Fe-starved leaves relative to control leaves (Fig. 2b), thus confirming the previous observations of Baxter *et al*. (2008a). The increased concentrations of K, Mg, Mn, Zn and Cu under Fe starvation indicate that these elements are dependent on Fe availability in leaves, whereas Mo nutrition had hardly any effect on these elements. Leaf Na contents were not affected by isolated Mo or Fe starvation, while the combined starvation resulted in elevated concentrations of Na. Finally, as observed in roots, Ca concentrations were not affected by the different nutritional deficiencies, although Ca quantification in this tissue was associated with the highest variation (Fig. 2b).

The observed Mo accumulation in roots occurring under Fe deprivation was attributable, in part, to a genuine increase in Mo uptake as the total Mo content in whole plants grown under Fe deprivation increased two-fold with respect to control plants (Table 1). This increase in Mo in roots is also attributable to the accumulation of Mo in roots at the expense of leaves; indeed, the Mo content was reduced in the stems of Fe-starved plants (Fig. S4). This increased Mo uptake took place from a medium that was progressively acidified by roots under Fe deprivation, regardless of the Mo concentration in the medium (Fig. S5). The strong acidification is well documented in cucumber (Dell'Orto *et al*., 2002) and in other plant species and is caused by the induction of H^+-ATPase activity as part of the strategy I Fe-deficiency response (Santi & Schmidt, 2009).

Table 1. Total molybdenum (Mo) and iron (Fe) contents in whole cucumber plants grown for 10 d under single or combined Mo and Fe starvation

	µg Mo g^{-1} DW	µg Fe g^{-1} DW
Control	13.839 ± 2.430	656.696 ± 61.143
−Mo	0.282 ± 0.036 **	435.903 ± 22.352 *
−Fe	29.606 ± 3.592 *	111.963 ± 14.645 **
−Mo−Fe	0.520 ± 0.205 **	124.012 ± 7.611 **

- Mo and Fe contents are shown in plants grown for 10 d in control hydroponic medium (+Mo+Fe), in medium devoid of Mo (−Mo), devoid of Fe (−Fe), or devoid of both micronutrients (−Mo−Fe). Each value is the mean ± SE of three independent samples, each containing a single whole plant. Significant differences with respect to controls in the same experimental conditions: **, $P < 0.01$; *, $P < 0.05$, according to Student's *t*-test.

Meanwhile, total Fe content was reduced in whole plants grown under Mo deprivation (Table 1). No alteration in Fe content was detected in either Mo-deficient roots or leaves (Fig. 2), and this decrease in total Fe content in Mo-starved whole plants is attributable to a decreased Fe content in the stem, that is, decreased transport of Fe through the xylem/phloem (Fig. S4).

Single or combined Mo and Fe starvation differentially impacts activities of molybdo-enzymes and Moco intermediates in roots and leaves

The activities of the molybdo-enzymes NR, SO, XDH and AO were measured in both roots and leaves. With SO as the only exception, the functionality of all these enzymes depends on additional Fe-containing cofactors (Bittner, 2014). Notable changes induced by Fe and/or Mo starvation were observed in both roots and leaves, albeit with opposite tendencies in some cases (Fig. 3). The most pronounced alterations were observed for NR, the activities of which were increased up to eight-fold in Fe-starved roots (Fig. 3a) but decreased to about the same degree in leaves (Fig. 3b). Mo starvation caused a doubling of root NR activity rather than a decrease. XDH activities were likewise altered in Fe-starved roots and leaves, but in the opposite direction compared with NR activities, as they decreased in roots and increased in leaves. In contrast to Fe starvation, Mo starvation had no significant effect (Fig. 3a) or only a marginally significant effect (Fig. 3b) on XDH activity in roots and leaves, respectively. Even though AO shares significant sequence similarity to XDH and harbours the same cofactors, its activity in leaves was strongly reduced by Fe starvation, which is in sharp contrast to the increased XDH activity under the same conditions (Fig. 3b). The decreased activity of AO in Fe-deficient leaves is in accordance with the higher water loss rate observed in Fe-starved plants after removal from hydroponic medium and wilting for 120 min (Fig. S6), in accordance with the crucial role of AO in abscisic acid biosynthesis. Irrespective of the applied treatment, AO activities in roots were too weak to allow densitometric monitoring of activity bands or interpretation of the respective activity-stained gels (Fig. S7). In roots, SO was the only molybdo-enzyme whose activity was significantly reduced by Mo starvation (Fig. 3a). Remarkably, Fe starvation alone in roots had no effect on SO activity, but in addition to Mo starvation appeared to rescue SO activity to control levels. In contrast to roots, SO activity in leaves was strongly stimulated by Fe starvation alone, with the combined starvation likewise reverting SO activity back to control levels (Fig. 3b), as observed in roots. All these results suggest that Mo and Fe availabilities in roots and leaves have differential effects on each individual molybdo-enzyme. The biologically active form of Mo, Moco, might be relocated between the different enzymes with its net amount being largely identical under all conditions.

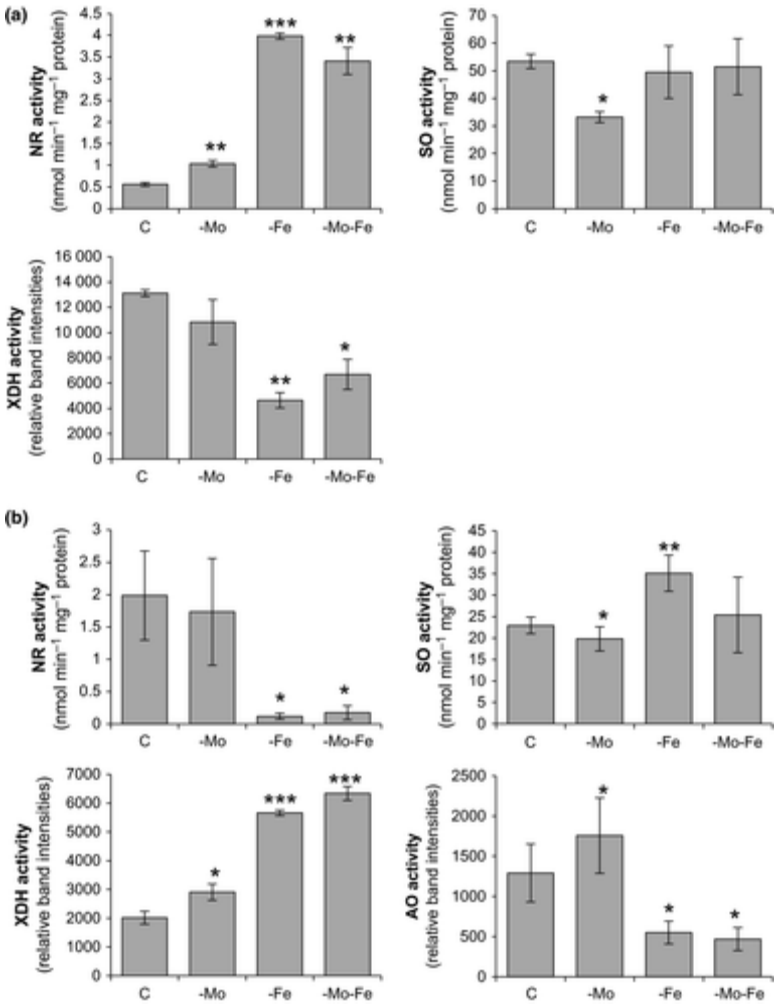

Figure 3

Open in figure viewerPowerPoint

Activities of molybdo-enzymes in cucumber plants grown under single or combined molybdenum (Mo) and iron (Fe) starvation. (a) Nitrate reductase (NR), xanthine dehydrogenase (XDH) and sulphite oxidase (SO) activities in roots from plants grown for 10 d in control (C) hydroponic medium (+Mo+Fe), and in medium devoid of Mo (−Mo), devoid of Fe (−Fe), or devoid of both micronutrients (−Mo−Fe). (b) NR, XDH, SO and aldehyde oxidase (AO) activities in leaves from plants grown as in (a). Bars represent mean values ± SE of three (NR in roots), three (SO in roots), three (XDH in roots), three (NR in leaves), four (SO in leaves), four (XDH in leaves), and four (AO in leaves) independent samples. Significant differences between treated samples and controls in the same experimental conditions: ***, $P < 0.0005$; **, $P < 0.005$; *, $P < 0.05$, based on Student's *t*-test.

Caption

To test this hypothesis, Moco and its ultimate Mo-free precursor MPT were converted into their common stable oxidation product FormA-dephospho, while the Moco intermediate cPMP was converted into the unique stable oxidation product CompoundZ. Subsequently, FormA-dephospho and CompoundZ were quantified in roots and leaves of plants grown under single or combined Mo and Fe starvation (Fig. 4), with FormA-dephospho representing the sum of Moco and MPT (Moco+MPT) and CompoundZ directly representing cPMP. Surprisingly, Mo starvation alone did not have any effect on the concentrations of Moco+MPT and cPMP, either in roots (Fig. 4a) or in leaves (Fig. 4b). By contrast, Fe starvation had a stimulating effect on the biosynthesis of cPMP and Moco+MPT in both roots and leaves, with isolated Fe starvation generally causing increasing

Moco+MPT and cPMP concentrations and combined Mo/Fe starvation having more differential effects. The latter was revealed by unaltered concentrations of Moco+MPT in Mo/Fe-starved roots (Fig. 4a), while Moco+MPT concentrations in leaves (Fig. 4b) and cPMP concentrations in both roots and leaves (Fig. 4a,b) were likewise increased. Nevertheless, these results clearly show that Fe availability strongly affects Moco biosynthesis, this effect already being obvious at the first step of Moco biosynthesis, namely cPMP synthesis.

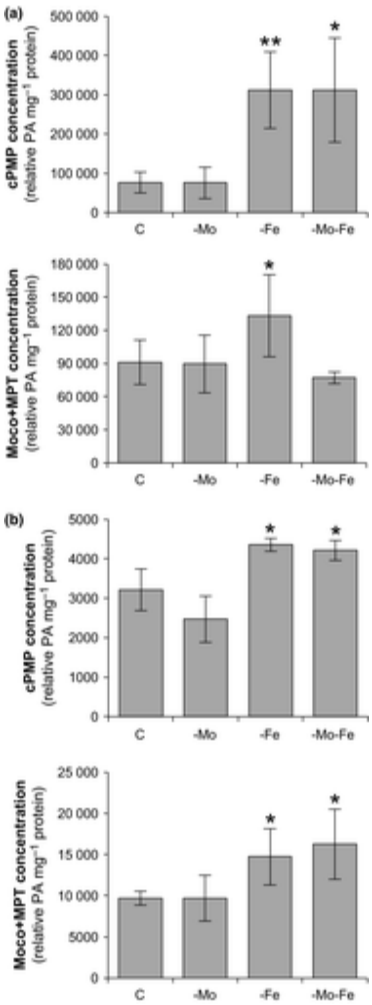

Figure 4

Open in figure viewerPowerPoint

Molybdenum cofactor (Moco) intermediates in cucumber plants grown under single or combined molybdenum (Mo) and iron (Fe) starvation. (a) Moco+MPT and cPMP concentration in roots from plants grown for 10 d in control (C) hydroponic medium (+Mo+Fe), and in medium devoid of Mo (−Mo), devoid of Fe (−Fe), or devoid of both micronutrients (−Mo−Fe). (b) Moco+MPT and cPMP concentration in roots from plants grown as in (a). Bars represent mean values ± SE of three to four independent samples for determination of cPMP and Moco+MPT concentration in roots and leaves. Significant differences between treated samples and controls in the same experimental conditions: **, $P < 0.01$; *, $P < 0.05$, based on Student's *t*-test.

Caption

Molybdenum content increases in Fe-deficient root mitochondria and Fe content increases in Mo-deficient root mitochondria

Mitochondria were purified from roots of plants grown under single and combined Mo and Fe starvation, with a protocol ensuring minimal peroxisomal contamination (Millar *et al*., 2007). Immunological analysis of the fractions obtained during the purification process, that is, total extract (TE), plastidial (P), mitochondrial (M) and peroxisomal (PX) fractions, confirmed a strong enrichment of mitochondria with negligible contamination when using antibodies against Toc33, porin and catalase as marker proteins for plastids, mitochondria and peroxisomes, respectively (Fig. S8). These mitochondrial fractions were used for profiling the ionomes and it turned out that single and combined Mo and Fe starvation was effective in altering Mo and Fe concentrations not only in root tissues, but also at the mitochondrial level (Fig. 5). Mo and Fe were indeed decreased in mitochondria from Mo- and Fe-starved roots, respectively.

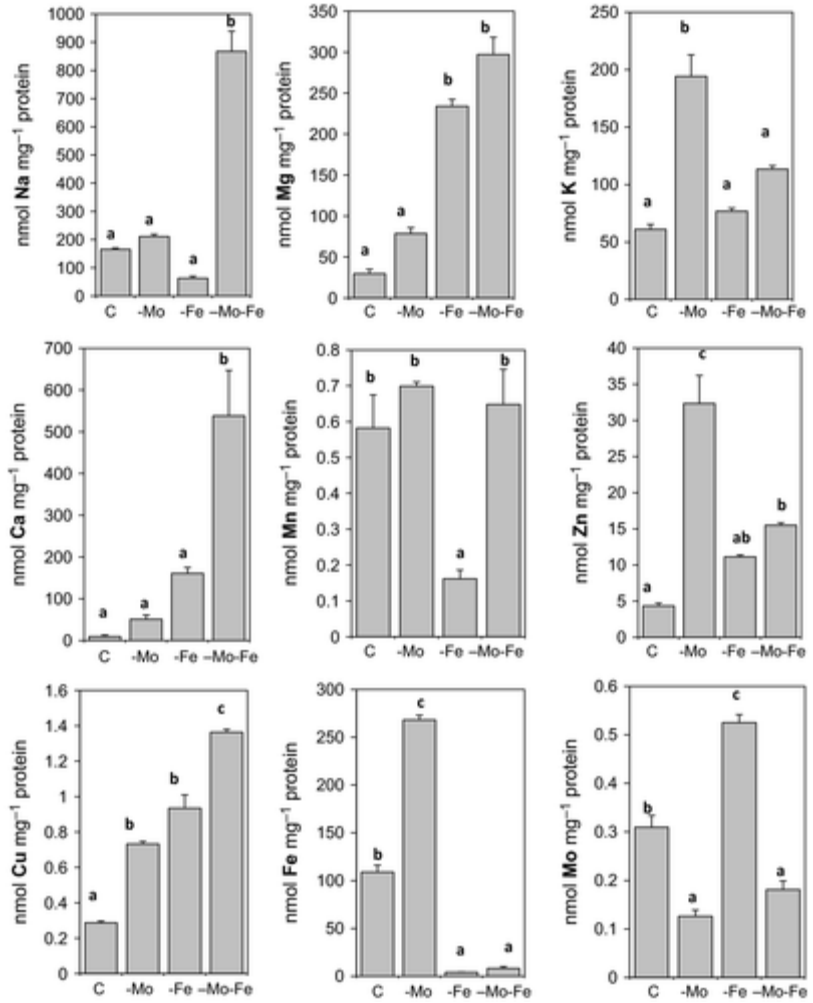

Figure 5

Open in figure viewerPowerPoint

Ionome of mitochondria purified from roots of cucumber plants grown for 10 d in control (C) hydroponic medium (+Mo+Fe), and in medium devoid of molybdenum (Mo) (−Mo), devoid of iron

(Fe) (−Fe), or devoid of both micronutrients (−Mo−Fe). Bars represent mean values ± SE of at least three independent samples. Different letters indicate statistically significant difference ($P < 0.05$).

Caption

Furthermore, Mo increased in Fe-deficient mitochondria and, reciprocally, Fe increased in Mo-deficient mitochondria. Taken together, ionomics on root tissues and on their mitochondria show that Fe starvation causes an increase of Mo in both whole root tissues and their mitochondria, whereas Mo starvation does not alter Fe content in whole root tissues but does alter the distribution of Fe to mitochondria, thus suggesting that Mo deficiency alters the subcellular Fe distribution.

Sodium and Ca contents were increased in −Mo−Fe mitochondria only; Mg content was affected solely by Fe starvation, regardless of Mo supply; K content increased in −Mo mitochondria only; a strong reduction of Mn was exclusively observed in −Fe mitochondria, as also observed in whole root tissues; Zn was highest in −Mo mitochondria; lastly, a three-fold increase of Cu concentration was observed in −Mo or −Fe mitochondria and a nearly five-fold increase under combined starvation (Fig. 5).

The most relevant biochemical and ionome changes occurring in cucumber roots and leaves under Mo or Fe starvation are summarized in Fig. S9.

Mitochondrial proteome profiles reveal the involvement of formate dehydrogenase (FDH) in the molecular crosstalk between Fe and Mo homeostasis

The protein profiles of mitochondria purified from roots of plants grown under single or combined Mo and Fe starvation were obtained by MudPIT technology (Delahunty & Yates, 2007; Cosentino *et al*., 2013), resulting in the identification of > 1400 proteins (Table S1), 66% of which were characterized by a total SpC ≥ 2.

Expression levels of 134 proteins were significantly altered in at least one of the reported nutritional conditions (Table S2) and their hierarchical clustering highlights two major groups of samples that depend on the Fe supply (Fe sufficiency vs Fe starvation) (Fig. 6), suggesting that Fe deprivation has a major impact on root cells, with respect to Mo deprivation, at least in our experimental conditions. In particular, 28 proteins were differentially expressed under Fe deficiency (Table 2); roughly half of them are associated with the respiratory chain and the TCA cycle, whereas the remaining proteins are associated with amino acid metabolism and other pathways. Higher expression of four proteins belonging to the branched chain amino acid catabolism process was observed, namely, methylcrotonyl-CoA carboxylase subunit alpha, lipoamide acyltransferase, dihydrolipoyl dehydrogenase and isovaleryl-CoA dehydrogenase (IVDH) (Table 2) (Peng *et al*., 2015). The last enzyme is of particular interest as it is defined as an alternative electron donor to the respiratory rate (Araulo *et al*., 2010).

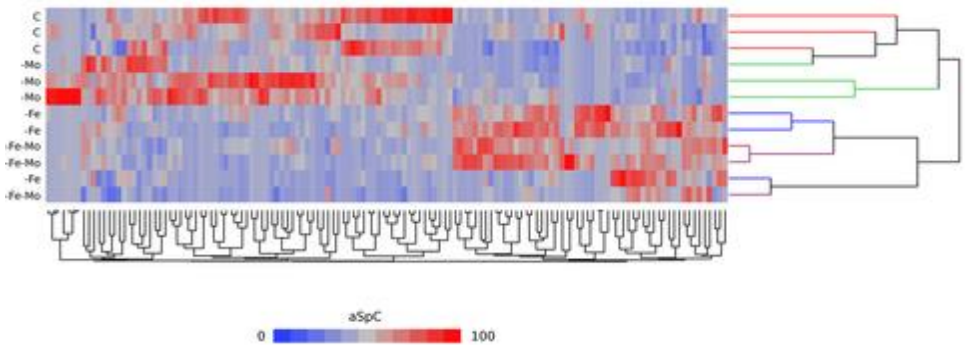

Figure 6

Open in figure viewerPowerPoint

Hierarchical clustering of proteins differentially accumulating in mitochondria purified from roots of cucumber plants grown for 10 d under control (C) hydroponic medium (+Mo+Fe) or under single or combined molybdenum (Mo) and iron (Fe) starvation. Clustering was performed by computing the average spectral count (aSpC) value of proteins selected by linear discriminant analysis (LDA); Euclidean's distance metric and Ward's method were applied. The heat map is related to the normalized aSpC (range 0–100) and indicates down- (blue) and up-regulated (red) proteins, respectively.

Caption

Table 2. Proteins differentially expressed, under iron (Fe) deficiency, in cucumber root mitochondria

NCBI ID	UNIPROT ID	Gene	Annotation	aSpC				DAve			Log_e(SpC ratio)		
				C	–Mo	–Fe	–Mo–Fe	C/–Mo	C/–Fe	C/–Mo–Fe	C/–Mo	C/–Fe	C/–Mo–Fe
Respiratory chain related proteins													
449451499	A0A0A0KJ15	Csa_6G501980	Probable NAD(P)H dehydrogenase (quinone) FQR1-	1	1.1	0.1	0.1		1.63	1.59		2.30	2.30

NCBI ID	UNIPROT ID	Gene	Annotation	aSpC				DAve			Log_e(SpC ratio)		
				C	C–Mo	C–Fe	C–Mo–Fe	C/C–Mo	C/C–Fe	C/C–Mo–Fe	C/C–Mo	C/C–Fe	C/C–Mo–Fe
			like 2										
449466103	A0A0A0L325	Csa_3G081930	Probable NAD(P)H dehydrogenase (quinone) FQR1-like 1	3.6	4.1	1	0.5		1.15	1.51		1.28	1.97
449467877	A0A0A0LDA2	Csa_3G845450	NADH dehydrogenase [ubiquinone] 1 alpha subcomplex subunit 2	1.6	1.9	0.8	0.7		0.66	0.76		0.69	0.83

NCBI ID	UNIPROT ID	Gene	Annotation	aSpC				DAve			Log_e(SpC ratio)		
				C	C–Mo	C–Fe	C–Mo–Fe	C/C–Mo	C/C–Fe	C/C–Mo–Fe	C/C–Mo	C/C–Fe	C/C–Mo–Fe
449470049	A0AA0ALP60	Csa_2G360050	Succinate dehydrogenase subunit 5, mitochondrial	16.6	15.9	11.3	12.7		0.37	0.26		0.38	0.27
449462912			Mitochondrial-processing peptidase subunit alpha	37.5	39.8	29.8	26.8		0.23	0.33		0.23	0.34
449434869	A0AA0KQD6	Csa_5G603950	Pyruvate dehydrogenase E1 component sub	9.8	11.3	7.8	5.4		0.22	0.58		0.23	0.60

NCBI ID	UNIPROT ID	Gene	Annotation	aSpC				DAve			Log_e(SpC ratio)		
				C	−Mo	−Fe	−Mo−Fe	C/−Mo	C/−Fe	C/−Mo−Fe	C/−Mo	C/−Fe	C/−Mo−Fe
			unit alpha, mitochondrial										
44946550			Mitochondrial-processing peptidase subunit alpha-like	10.9	13.1	16.8	16.2		−0.43	−0.39		−0.43	−0.40
44943624 3	A0A0A0K6P2	Csa_7G429590	Citrate synthase, mitochondrial	23	20.4	37.4	39.5		−0.47	−0.52		−0.49	−0.54
44944429 8	A0A0A0KGA1	Csa_6G135470	Succinate-semialdehyde	6.1	6.4	11	11		−0.57	−0.56		−0.59	−0.59

NCBI ID	UNIPROT ID	Gene	Annotation	aSpC				DAve			Log_e(SpC ratio)		
				C	−Mo	−Fe	−Mo−Fe	C/−Mo	C/−Fe	C/−Mo−Fe	C/−Mo	C/−Fe	C/−Mo−Fe
			dehydrogenase, mitochondrial										
449454612			NAD-dependent malic enzyme 2, mitochondrial-like	5.8	5.1	11.2	8.4		−0.64	−0.38		−0.66	−0.37
449470271			Succinate dehydrogenase assembly factor 2, mitoch	0.2	0	0.7	0.7		−1.21	−1.18		−1.25	−1.25

NCBI ID	UNIPROT ID	Gene	Annotation	aSpC				DAve			Log_e(SpC ratio)		
				C	−Mo	−Fe	−Mo−Fe	C/−Mo	C/−Fe	C/−Mo−Fe	C/−Mo	C/−Fe	C/−Mo−Fe
			mitochondrial										
34668358	G3EIX2	cox1	Cytochrome c oxidase subunit 1 (mitochondrion)	0.2	0	0.8	0.4		−1.29	−0.75		−1.39	−0.69
44945769 0	A0A0A0LV07	Csa_1G071890	External alternative NAD(P)H-ubiquinone oxidoreductase B2, mitochondrial	0	0	1.3	1.8		−2	−2		−100	−100

NCBI ID	UNIPROT ID	Gene	Annotation	aSpC				DAve			Log_e(SpC ratio)		
				C	C/−Mo	C/−Fe	C/−Mo−Fe	C/−Mo	C/−Fe	C/−Mo−Fe	C/−Mo	C/−Fe	C/−Mo−Fe
4494463099			NADH dehydrogenase [ubiquinone] 1 alpha subcomplex assembly factor 3-like	0	0.1	0.5	0		−2			−100	
Amino acid metabolism													
4494503499	A0A0A0LN17	Csa_2G351700	Glycine dehydrogenase (decarboxylating), mitochondrial	30	34.5	23.2	21.4		0.25	0.33		0.26	0.34

NCBI ID	UNIPROT ID	Gene	Annotation	aSpC				DAve			Log_e(SpC ratio)		
				C	−Mo	−Fe	−Mo−Fe	C/−Mo	C/−Fe	C/−Mo−Fe	C/−Mo	C/−Fe	C/−Mo−Fe
4494415122	A0A0A0K7C2	Csa_6G000100	Dihydrolipoyldehydrogenase, mitochondrial-like	20.8	20.8	26.8	24.7		−0.25			−0.25	
4494429333			Aldehyde dehydrogenase family 2 member B4, mitochondrial-like	25.1	29.9	49.6	46.1		−0.65	−0.59		−0.68	−0.61
4494636855			Isovaleryl-CoA dehydroge	1.9	2	4	3.4		−0.74	−0.59		−0.74	−0.58

NCBI ID	UNIPROT ID	Gene	Annotation	aSpC				DAve			Log_e(SpC ratio)		
				C	−Mo	−Fe	−Mo−Fe	C/−Mo	C/−Fe	C/−Mo−Fe	C/−Mo	C/−Fe	C/−Mo−Fe
			nase, mitochondrial-like										
449460004	A0A0A0KVA1	Csa_4G056830	Gamma aminobutyrate transaminase 1, mitochondrial-like	13.3	12.7	31	30.6	−0.8	−0.79		−0.85	−0.83	
449458468	A0A0K5L0	Csa_7G387180	Methylcrotonoyl-CoA carboxylase subunit alpha, mitochond	1.8	2.1	5.6	4	−1.03	−0.77		−1.13	−0.80	

NCBI ID	UNIPROT ID	Gene	Annotation	aSpC				DAve			Log_e(SpC ratio)		
				C	−Mo	−Fe	−Mo−Fe	C/−Mo	C/−Fe	C/−Mo−Fe	C/−Mo	C/−Fe	C/−Mo−Fe
			rial isoform X1										
44946944	A0A0A0LW34	Csa_1G045490	Probable aldehyde dehydrogenase	2.3	2.5	7.4	6.3		−1.04	−0.92		−1.17	−1.01
44945960 2	A0A0A0KYN6	Csa_4G192110	Glutamate dehydrogenase 1	2.1	2.4	10.7	11.7		−1.35	−1.4		−1.63	−1.72
44943287 4	A0A0A0L5U6	Csa_3G164470	Lipoamide acyltransferase component of branched-chain	2.3	2.7	13.1	12.5		−1.41	−1.38		−1.74	−1.69

NCBI ID	UNIPROT ID	Gene	Annotation	aSpC				DAve			Log_e(SpC ratio)		
				C	−Mo	−Fe	−Mo−Fe	C/−Mo	C/−Fe	C/−Mo−Fe	C/−Mo	C/−Fe	C/−Mo−Fe
			alpha-ketoacid dehydrogenase complex, mitochondrial										
4494425699	A0A0A0M2W0	Csa_1G617370	Serine–glyoxylate aminotransferase	0	0	0.7	0		−2			−1000	
Other proteins													
2066041733	B6DQ61		Glutathione peroxidase, partial	0	0.2	0.6	0.9		−2	−2		−1000	−100

NCBI ID	UNIPROT ID	Gene	Annotation	aSpC				DAve			Log_e(SpC ratio)		
				C	−Mo	−Fe	−Mo−Fe	C/−Mo	C/−Fe	C/−Mo−Fe	C/−Mo	C/−Fe	C/−Mo−Fe
4494565332			Hydroxyacyl-glutathione hydrolase 3, mitochondrial-like	0	0	1.1	0.6		−2	−2		−100	−100
4494487844			Peroxidase 53-like	0	0.1	0.3	1.1		−2	−2		−100	−100
4494414500	A0A0A0K9Z6	Csa_6G004600	Bifunctional L-3-cyanoalanine synthase/cysteine synthase 1, mitoch	3	2.6	8	9.8		−0.9	−1.06		−0.98	−1.18

NCBI ID	UNIPROT ID	Gene	Annotation	aSpC				DAve			Log_e(SpC ratio)		
				C	−Mo	−Fe	−Mo−Fe	C/−Mo	C/−Fe	C/−Mo−Fe	C/−Mo	C/−Fe	C/−Mo−Fe
			mitochondrial										

- Proteins were identified by MudPIT (Multidimensional Protein Identification Technology) proteomic analysis of mitochondria purified from roots of cucumber plants grown for 10 d in control medium C (+Mo +Fe), and in medium devoid of molybdenum (Mo) (−Mo), devoid of Fe (−Fe), or devoid of both micronutrients (−Mo−Fe). aSpC, average spectral count; +Mo+Fe (control), $n = 6$; −Mo+Fe, $n = 6$; +Mo−Fe, $n = 8$; −Mo−Fe, $n = 7$. Proteins were selected by linear discriminant analysis (LDA) ($P < 0.05$) and pairwise comparisons between control condition C and a given deficiency condition D were further evaluated using the DAve index (aSpC_C − aSpC_D)/(aSpC_C + aSpC_D)/0.5), where SpC_C and SpC_D are the spectral counts in control (C) and any D condition (−Mo, −Fe, or −Mo−Fe). Fold change was estimated by using the natural logarithm (log_e) of the spectral count ratio aSpC_C/aSpC_D. Positive values of DAve and/or spectral count ratios indicate up-regulation in control C, while negative values of DAve and/or spectral count ratios indicate up-regulation in the deficiency condition D. For a given protein and its pairwise comparison in C with D, the DAve values are conventionally set at either +2 or −2, in case such a protein has been exclusively identified in either C or D, while the value of the natural logarithm of the spectral count ratio for the same proteins is conventionally set to 100 and −100, respectively. Missing DAve values (and spectral count ratios) indicate that they are not statistically significant.

The mitochondrial catabolism of some branched chain amino acids, such as lysine, methionine and threonine, can provide electrons to the IVDH enzyme and in turn to the electron-transfer flavoprotein:ubiquinone oxidoreductase system (ETFQO), which is a further alternative pathway for the transfer of electrons to the ubiquinone pool. At the same time, such a pathway would provide a precursor to sustain the TCA cycle (Peng *et al*., 2015).

Ten proteins were up-regulated under Mo deficiency only (Table 3) and seven of them (cinnamate-4-hydroxylase, trans-cinnamate-4-monooxygenase-like, cytochrome b5 isoform B, calnexin, calreticulin, reticulon and delta sterol reductase) are either localized to or associated with the endoplasmic reticulum (ER) and act in different cellular pathways, from lipid biosynthesis to Ca^{2+} homeostasis (Muller-Taubenberger *et al*., 2001; Ro *et al*., 2001; Nziengui *et al*., 2007; Kumar *et al*., 2012; Silvestro *et al*., 2013). A tight association between the ER and mitochondria might therefore occur under Mo deprivation. This association has already been documented and related to the biological network of cell death signalling (Grimm, 2012). Another possibility which would explain these results is that the localization of these seven proteins becomes mitochondrial under Mo deficiency.

Table 3. Proteins differentially expressed under molybdenum (Mo) deficiency

NCBI ID	UNIPROT ID	Gene	Annotation	aSpC				DAve			Log2(SpC ratio)		
				C	C–Mo	C–Fe	C–Mo–Fe	C/C–Mo	C/C–Fe	C/C–Mo–Fe	C/C–Mo	C/C–Fe	C/C–Mo–Fe
449438803	A0A0A0KZ82	Csa_4G103350	Delta(24)-sterol reductase-like lipid metabolisms	0.3	0.6	0	0	–0.81			–0.69		
449454792			calnexin homolog 1-like	0.2	0.7	0	0	–1.24			–1.25		
449454026	A0A0A0LFZ8	Csa_2G033940	Calreticulin	0.2	0.9	0	0	–1.17			–1.50		
449432104	A0A0A0L627	Csa_3G121020	Reticulon-like protein B1	0.2	0.9	0.1	0.1	–1.17			–1.50		
449467513			trans-cinnamate 4-	0.1	0.9	0	0	–1.49			–2.20		

NCBI ID	UNIPROT ID	Gene	Annotation	aSpC				DAve			Log2(SpC ratio)		
				C	–Mo	–Fe	–Mo–Fe	C/–Mo	C/–Fe	C/–Mo–Fe	C/–Mo	C/–Fe	C/–Mo–Fe
			monooxygenase-like										
1097154 82	Q17UC0	c4H	Cinnamate-4-hydroxylase	0	0.5	0	0	–2			–100		
4494324 22			cytochrome b5 isoform B-like linked to fatty acid desaturase	0	0.8	0	0.1	–2			–100		
4494327 33	A0A0A0L5N4	Csa_3G149980	Basic 7S globulin-like	0	1.1	0	0	–2			–100		
4494936	A0A0A0	Csa_7G	Vicianin hydr	0	0.7	0	0	–2			–1		

NCBI ID	UNIPROT ID	Gene	Annotation	aSpC				DAve			Log_e(SpC ratio)		
				C	−Mo	−Fe	−Mo−Fe	C/−Mo	C/−Fe	C/−Mo−Fe	C/−Mo	C/−Fe	C/−Mo−Fe
255	K9V3	428990	olase								00		
44943648 1	A0A0A0K996	Csa_7G398090	Indole-3-acetic acid-induced protein ARG2 involved in arginine biosynthesis	0	0.5	0	0.1	−2			−100		

- Proteins were identified by MudPIT proteomic analysis of mitochondria purified from roots of cucumber plants grown for 10 d in control medium C (+Mo +Fe), and in medium devoid of Mo (−Mo), devoid of iron (Fe) (−Fe), or devoid of both micronutrients (−Mo−Fe). aSpC, average spectral count; +Mo+Fe (control), $n = 6$; −Mo+Fe, $n = 6$; +Mo−Fe, $n = 8$; −Mo−Fe, $n = 7$. Proteins were selected by linear discriminant analysis (LDA) ($P < 0.05$) and pairwise comparisons between control condition C and a given deficiency condition D were further evaluated using the DAve index (aSpC_C − aSpC_D)/(aSpC_C + aSpC_D)/0.5), where SpC_C and SpC_D are the spectral counts in control (C) and in any D condition (−Mo, −Fe, or −Mo−Fe). Fold change was estimated by using the natural logarithm (log_e) of the spectral count ratio aSpC_C/aSpC_D. Positive values of DAve and/or spectral count ratios indicate up-regulation in control C, while negative values of DAve and/or spectral count ratios indicate up-regulation in the deficiency condition D. For a given protein and its pairwise comparison in C with D, the DAve values are conventionally set at either +2 or −2, in case such a protein has been exclusively identified in either C or D, while the value of the natural logarithm of the spectral count ratio for the same proteins is conventionally set to 100 and −100, respectively. Missing DAve values (and spectral count ratios) indicate that they are not statistically significant.

Molybdenum and Fe deficiencies had opposite effects on the expression of 18 mitochondrial proteins (Table 4), among which is formate dehydrogenase (FDH). This protein catalyses the oxidation of the formate ion to carbon dioxide, coupled with the reduction of NAD^+ to NADH (Alekseeva *et al*., 2011). Bacterial FDH can bind Mo whereas the plant FDH, localized in the mitochondria, cannot. FDH is one of the most abundant proteins in potato (*Solanum tuberosum*) tuber mitochondria (Havelund *et al*., 2013) and its accumulation is induced by a variety of stresses (Alekseeva *et al*., 2011), including Fe deficiency (Herbik *et al*., 1996; Suzuki *et al*., 1998; Itai *et al*., 2013). In cucumber, FDH is encoded by a single gene expressed as three alternatively spliced transcripts (Cucsa 3393670.1, Cucsa 3393670.2 and Cucsa 3393670.3) and the protein identified in the present study corresponds to Cucsa 3393670.1.

Table 4. Proteins with opposite expression under molybdenum (Mo) and iron (Fe) deficiencies

NCBIID	UNIPROTID	Gene	Annotation	aSpC				DAve			Log_e(SpC ratio)		
				C	−Mo	−Fe	−Mo−Fe	C/−Mo	C/−Fe	C/−Mo−Fe	C/−Mo	C/−Fe	C/−Mo−Fe
449455056	A0AA0LVG1	Csa_1G527890	Mitochondrial import inner membrane translocase subunit TIM10	0.5	0	1.7	0.6	2	−1.14	−0.29	100	−1.22	−0.18
4494672241			Major allergen Pru ar 1-like	0.5	0	1.6	2.4	2	−1.1	−1.36	100	−1.16	−1.57
8947487 3	Q7Y1B3	aox2	Mitochondrial alternative oxidase 2	0.3	0	1	1.4	2	−1.05	−1.24	100	−1.20	−1.54

NCBIID	UNIPROTID	Gene	Annotation	aSpC				DAve			Log_e(SpC ratio)		
				C	−Mo	−Fe	−Mo−Fe	C/−Mo	C/−Fe	C/−Mo−Fe	C/−Mo	C/−Fe	C/−Mo−Fe
449517517			uncharacterized LOC101205546	0.3	0	0.7	0.5	2	−0.68	−0.37	100	−0.85	−0.51
449433571			solanesyl diphosphate synthase 3, chloroplastic/mitochondrial-like	0.6	0.1	1.6	1.7	1.21	−0.93	−0.98	1.79	−0.98	−1.04
449462360	A0A0A0KT33	Csa_5G317890	Probable acyl-activating enzyme 5, peroxisomal	0.4	0.1	1.3	1.5	1.02	−0.95	−1.08	1.39	−1.18	−1.32
449444399			external alternative NAD(P)H-ubiquinone oxidoreductase B2, mitoch	0.3	0.1	1.7	2.9	0.71	−1.4	−1.62	1.10	−1.73	−2.27

NCBIID	UNIPROTID	Gene	Annotation	aSpC				DAve			Log$_e$(SpC ratio)		
				C	−Mo	−Fe	−Mo−Fe	C/−Mo	C/−Fe	C/−Mo−Fe	C/−Mo	C/−Fe	C/−Mo−Fe
			ondrial-like										
1675982500	B7SIS4		6,7-Dimethyl-8-ribityllumazine synthase	0.6	0.2	7.5	3.9	1.01	−1.7	−1.46	1.10	−2.53	−1.87
4494466600	A0A0A0LHY6	Csa_3G836500	Formate dehydrogenase, mitochondrial	25.8	9.6	117.4	165.8	0.91	−1.28	−1.46	0.99	−1.52	−1.86
3132255252	Q7Y1A3		Alternative oxidase, partial	2.8	1.5	6.1	7.1	0.62	−0.74	−0.87	0.62	−0.78	−0.93
4494500700	A0A0A0KSE3	Csa_5G523030	Altered inheritance of mitochondrial protein 32	2.3	1.9	5.6	4.3	0.21	−0.84	−0.6	0.19	−0.89	−0.63

NCBIID	UNIPROTID	Gene	Annotation	aSpC				DAve			Log$_e$(SpC ratio)		
				C	–Mo	–Fe	–Mo–Fe	C/–Mo	C/–Fe	C/–Mo–Fe	C/–Mo	C/–Fe	C/–Mo–Fe
449431926			Cytochrome c1-1, heme protein, mitochondrial-like	16.6	20.5	13.2	12.4	–0.21	0.23	0.29	–0.21	0.23	0.29
449457544	A0AA0AKY37	Csa_4G047340	Pyridine nucleotide-disulfide oxidoreductase domain-containing protein 2-like	1.1	1.4	0.5	0.1	–0.23	0.69	1.61	–0.24	0.79	2.40
449434468			Aspartic proteinase-like protein 1-like	1.7	2.2	0.5	0.6	–0.24	1.16	0.96	–0.26	1.22	1.04
449470453	A0AA0AL2E3	Csa_3G077600	Calcium-dependent protei	0.5	0.9	0	0	–0.56	2	2	–0.59	100	100

NCBIID	UNIPROTID	Gene	Annotation	aSpC				DAve			Log$_e$(SpC ratio)		
				C	−Mo	−Fe	−Mo−Fe	C/−Mo	C/−Fe	C/−Mo−Fe	C/−Mo	C/−Fe	C/−Mo−Fe
			n kinase-like										
449442389			elongation factor 1-alpha	11.5	22.8	5	7	−0.66	0.79	0.48	−0.68	0.83	0.50
449479051			Uncharacterized protein LOC101232327	3.1	7.2	0.1	1.9	−0.8	1.85	0.49	−0.84	3.43	0.49
449438929			Epidermis-specific secreted glycoprotein EP1-like	0.7	2.5	0	0	−1.09	2	2	−1.27	100	100

- Proteins were identified by MudPIT proteomic analysis of mitochondria purified from roots of cucumber plants grown for 10 d in control medium C (+Mo +Fe), and in medium devoid of Mo (−Mo), devoid of Fe (−Fe), or devoid of both micronutrients (−Mo−Fe). aSpC, average spectral count; +Mo+Fe (control), $n = 6$; −Mo+Fe, $n = 6$; +Mo−Fe, $n = 8$; −Mo−Fe, $n = 7$. Proteins were selected by linear discriminant analysis (LDA) ($P < 0.05$) and pairwise comparisons between control condition C and a given deficiency condition D were further evaluated using the DAve index (aSpC_C − aSpC_D)/(aSpC_C + aSpC_D)/0.5), where SpC_C and SpC_D are the spectral counts in control (C) and in any D condition (−Mo, −Fe, or −Mo−Fe). Fold change was estimated by using the natural logarithm ($\log_e$) of the spectral count ratio aSpC_C/aSpC_D. Positive values of DAve and/or spectral count ratios

indicate up-regulation in control C, while negative values of DAve and/or spectral count ratios indicate up-regulation in the deficiency condition D. For a given protein and its pairwise comparison in C with D, the DAve values are conventionally set at either +2 or −2, in case such a protein has been exclusively identified in either C or D, while the value of the natural logarithm of the spectral count ratio for the same proteins is conventionally set to 100 and −100, respectively. Missing DAve values (and spectral count ratios) indicate that they are not statistically significant.

Among the proteins with opposite expression under Mo and Fe deficiencies, seven are associated with the respiratory chain and TCA cycle pathways (Table 4). Alternative oxidase subunits, external NAD(P)H ubiquinone oxidoreductase B2 and solanesyl diphosphate synthase 3 (probably involved in ubiquinone biosynthesis) were up-regulated under Fe deficiency and down-regulated under Mo deficiency. However, pyridine nucleotide-disulphide oxidoreductase domain containing protein 2-like and epidermis-specific secreted glycoprotein EP1-like were down-regulated under Fe deficiency and up-regulated under Mo deficiency.

Furthermore, 6,7-dimethyl-8-ribityllumazine (DMRL) synthase accumulated under Fe deficiency and decreased under Mo deficiency; this enzyme catalyses the penultimate step of riboflavin (vitamin B2) biosynthesis and its strong induction in Fe-deficient plants has been demonstrated previously (Rellán-Álvarez *et al*., 2010). Although 'ex novo' biosynthesis of vitamin B2 is localized to chloroplasts (Gerdes *et al*., 2012), its salvage and repair mechanisms may be spread across multiple organelles, in a so-called 'division of labour', which would allow the organelles to share the costs of processing and recycling of damaged metabolites (Colinas & Fitzpatrick, 2015).

Opposite expression under Mo and Fe deficiencies was observed for the mitochondrial import inner membrane translocase TIM10 (translocase inner membrane), elongation factor 1 alpha and aspartic-proteinase like1, suggesting that these deficiencies differentially impact protein import, translation and degradation in mitochondria.

Molybdenum and the molybdo-enzyme ARC accumulate in membranes of Fe-deficient root mitochondria

Mitochondria purified from cucumber roots of plants grown under either Mo or Fe starvation were further fractioned into the soluble (MSF) and the membrane (MMF; inner and outer) fractions. Mo increased in the membranes of Fe-deficient mitochondria (Fig. 7a). Also, Fe increased in the membranes of Mo-deficient mitochondria (Fig. 7b). The observed increase of Mo in the MMF fraction of the Fe-deficient mitochondria was accompanied by a higher accumulation of the Mo-enzyme mARC, as demonstrated by western blot analysis of MMF fractions with two antibodies raised against the Arabidopsis mARC-1 and mARC-2 isoforms, which show enhanced accumulation of a protein of the expected size (*c*. 60 kDa) for the mARC dimer (Fig. 7c).

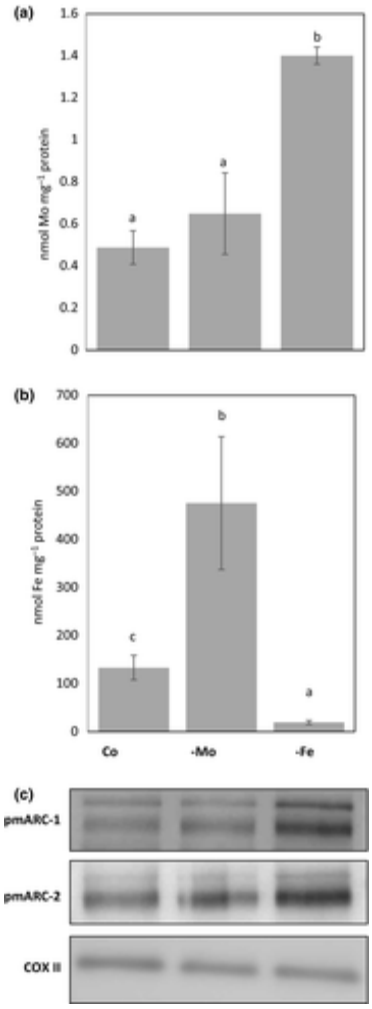

Figure 7

Open in figure viewerPowerPoint

Molybdenum (Mo) and iron (Fe) contents and mitochondrial amidoxime reducing component (mARC) expression in the membrane fractions of root mitochondria. (a) Mo content and (b) Fe content in membrane fractions of mitochondria purified from roots of cucumber plants grown for 10 d in control (C) hydroponic medium, or in hydroponic medium under Mo (−Mo) or Fe starvation (−Fe). Bars represent mean values ± SE of two samples. Different letters indicate statistically significant difference ($P < 0.05$). (c) Western blot analysis of membrane fractions of root mitochondria purified as in (a, b), using polyclonal antibodies against Arabidopsis mARC-1 and mARC-2. Six μg of proteins was loaded in each lane; equal loading of proteins was confirmed with the polyclonal antibody against mitochondrial cytochrome c oxidase subunit II (COX II)**.**

Caption

Discussion

Interactions occur among the homeostatic controls of various nutrients in plants (Forieri *et al*., 2013; Briat *et al*., 2015b; Zuchi *et al*., 2015). However, the molecular crosstalk between Mo and Fe homeostases has been little investigated and evidence for its existence is mostly circumstantial (Bittner, 2014).

The present work explored the effects of combined Mo and Fe starvation and the ionomes and proteomes of Mo and/or Fe-deficient mitochondria.

Fe starvation, which leads to plant Fe deficiency, had a clear impact on Mo distribution in roots and leaves, causing an increase in Mo in roots (and in their mitochondria) and a decrease in Mo in leaves. The observed Mo increase in −Fe roots, which strongly acidified the hydroponic medium as part of the strategy I Fe-deficiency response, was attributable to increased Mo uptake from the medium and not only to reduced Mo transport from roots to leaves. This result was unexpected as, on one hand, soil acidification below a pH of 5.5 is well known to decrease the molybdate uptake rate and thus is more likely to be accompanied by typical Mo-deficiency symptoms (Kaiser *et al*., 2005), while, on the other hand, the increase in pH by liming can remediate Mo-deficiency symptoms and molybdate concentration in plants. Our results may imply that Fe deficiency has a major impact on Mo homeostasis not only by triggering the molybdate uptake by yet unknown mechanisms, but also by neutralizing the molecular elements that usually impair molybdate uptake in a pH-dependent manner.

Impact of Fe and Mo deficiencies on molybdo-enzymes

As well as affecting Mo homeostasis in terms of element uptake and distribution, Fe deficiency affects overall Mo metabolism: cPMP and Moco biosyntheses are increased, possibly as a result of a tissue-specifically increased demand for certain molybdo-enzymes, such as NR in roots and XDH in leaves. Such an increase of NR activity in Fe-deficient roots is in agreement with an increased concentration of amino acids as observed in the xylem sap of Fe-deficient cucumber plants (Borlotti *et al*., 2012). A leaf-specific increase of XDH activity, however, might be explained by stress-induced senescence caused by Fe deficiency. Not only natural leaf senescence (Hesberg *et al*., 2004; Nakagawa *et al*., 2007) but also dark-induced leaf senescence (Brychkova *et al*., 2008) is accompanied by strongly enhanced XDH activity. Nevertheless, the question remains of why NR and XDH, which are both involved in nitrogen metabolism, are inversely regulated under Fe deficiency. A possible explanation is related to the rather diverse specifications of these two proteins: while increasing NR activities might meet the demand of enhanced nitrogen assimilation in Fe-starved roots, XDH might compensate for the simultaneous reduction of NR activity in leaves and provide nitrogen compounds to related pathways in leaves via the degradation of purines.

We propose that the rearrangement of Mo metabolism occurring under Fe deficiency has the aim of redistributing the residual Fe content and the increased Moco content to potentiate NR activity in roots (Fig. 8). Under Fe deprivation, nitrogen assimilation would therefore largely occur in roots to circumvent the severe functional impairment of leaves under such a nutritional deficiency (Borlotti *et al*., 2012).

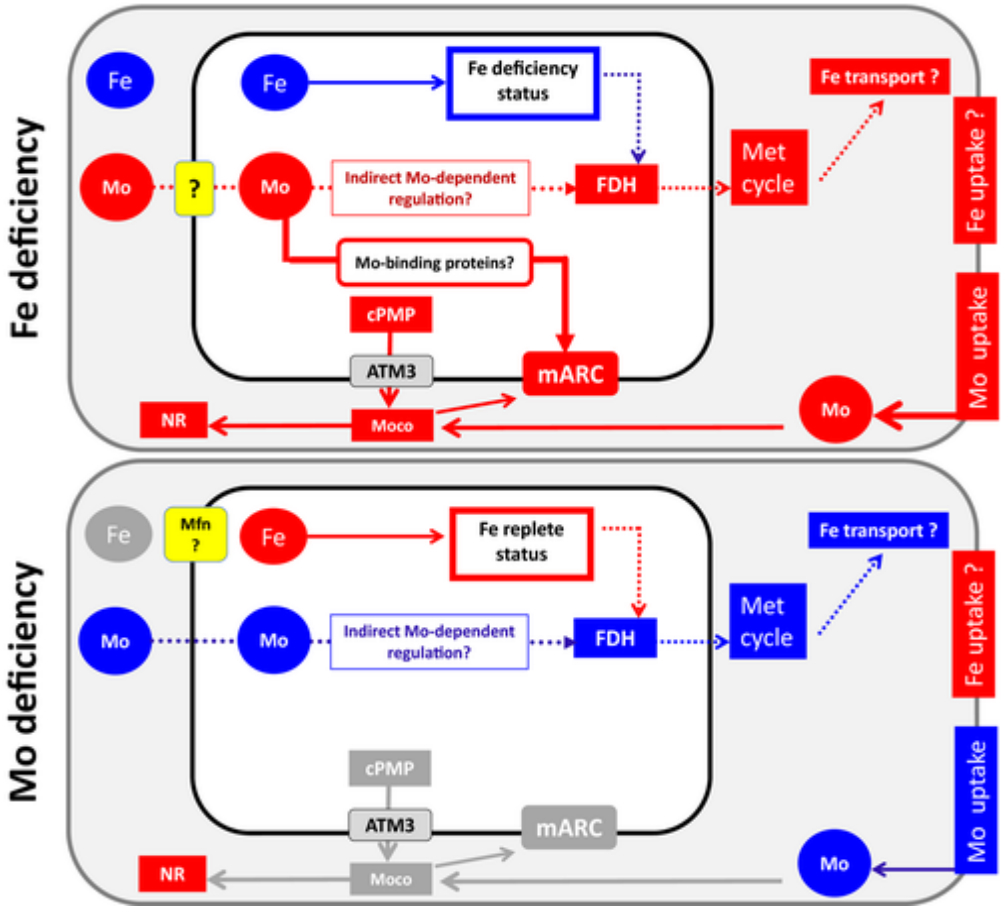

Figure 8

Open in figure viewerPowerPoint

Main changes in and novel hypothetical scenarios for iron (Fe) and molybdenum (Mo) homeostasis, occurring under Fe and Mo deficiencies in root cells. Upper panel: under Fe deficiency, Mo accumulates in root cells and in their mitochondria. Such accumulation is a consequence of enhanced Mo uptake. The increased Mo content triggers, in turn, molybdenum cofactor (Moco) biosynthesis and nitrate reductase (NR) activity. The Fe deficiency status, in the cell and within the mitochondria, triggers an up-regulation of formate dehydrogenase (FDH) that can positively act on the Met cycle. An indirect Mo-dependent regulation of FDH protein expression is suggested. The question mark in yellow (upper panel) refers to the still unknown mitochondrial Mo transporter. Mo-binding proteins represent a set of putative proteins that are capable of binding molybdenum or molybdate. The function of these proteins might be to store and/or transfer Mo between the site of delivery and sites of consumption (proteins with this function exist in prokaryotes); thus, in plants, a putative function might also be to shuttle Mo/molybdate between compartments. Mitochondrial amidoxime reducing component (mARC) accumulate in membranes. Lower panel: under Mo deficiency, Fe accumulates in mitochondria. Molybdenum deficiency causes, as a consequence, a down-regulation of FDH expression, with a negative effect on Fe transport, through the Met cycle. Mfl is a hypothetical mitoferrinlike transporter, responsible for Fe transport within mitochondria. Dotted lines underline hypothetical scenarios suggested in this work while continuous lines link the results obtained in this work. Blue and red colours indicate, respectively, decreased and increased values, with respect to control plants (+Mo+Fe).

Caption

SO is the only molybdo-enzyme whose activity decreases in both Mo-deficient roots and leaves, in agreement with the finding that SO is the only molybdo-enzyme not requiring Fe as a cofactor. It is

thus concluded that SO activity and SO protein levels are directly correlated with the availability of Mo, in the form of Moco, which affects both of them. In contrast, the results obtained do not allow us to correlate NR, XDH, and AO activities with their respective protein levels. On one hand, their activities indeed depend on the availability of Mo-, Fe- and flavin-dependent cofactors, which all appeared to be affected in the present study. On the other hand, all these proteins typically undergo co- or posttranslational modifications such as phosphorylation (NR), ubiquitination (AO) or Moco sulphuration (AO and XDH), respectively (Bittner & Mendel, 2010), which have a strong impact on the proteins' activities even without affecting protein levels.

The purification of root mitochondria and the analysis of their fractions showed that both Mo and Fe accumulate in the membranes of Fe- and Mo- deficient mitochondria, respectively. Such findings are in accordance with the observed increase in mARC in the membranes of Fe-deficient root mitochondria and open the way to a more focused search for the *in vivo* role of mARC enzymes in plants.

Impact of Fe and Mo deficiencies on mitochondrial ionome and proteome

Mitochondria mediate Fe deficiency-induced metabolic responses in plants (Vigani, 2012) and the impact of Fe and Mo deficiencies on both the ionomes and the proteomes of these organelles are explored in this work. The putative cucumber orthologue of Arabidopsis MOT1 (XP_004138873) could not be identified as part of such a mitochondrial proteome. This observation is challenging, as the precise subcellular localization of MOT1 is still unresolved (Tomatsu *et al*., 2007; Baxter *et al*., 2008b). However, low-abundance proteins as well as mitochondrial transporters, such as ferritin (Vigani *et al*., 2013b) and ATM3 (Teschner *et al*., 2010), respectively, are part of the full list of proteins constituting the mitochondrial proteome (Table S1; NCBI 449460884 and NCBI 449444328, respectively). Notably, ferritin accumulates in cucumber mitochondria under Fe excess, whereas under Fe sufficiency its levels are low, although detectable (Vigani *et al*., 2013b). Therefore, lack of identification of MOT1 could further validate its nonmitochondrial localization, as proposed by Tomatsu *et al*. (2007). The transport mechanism of Mo into mitochondria still remains unresolved (Fig. 8).

The finding that FDH is among the mitochondrial proteins displaying opposite regulation under Mo and Fe deficiencies is interesting. FDH is an enigmatic enzyme (Havelund *et al*., 2013), which has been proposed as an ancillary enzyme of the methionine cycle pathway, through which Met is supplied for synthesis of ethylene (Miyazaki & Yang, 1987) and for the biosynthesis of nicotianamine and mugeinic acids. Nicotianamine is a well-established Fe-chelator for phloematic Fe transport and distribution in plants, and also has a proposed signalling role in the regulation of Fe deficiency-inducible genes (Kobayashi *et al*., 2005; Itai *et al*., 2013; Kobayashi & Nishizawa, 2014). Results obtained in the present work suggest that a reduction of the Fe content occurs in phloem/xylem under Mo starvation. Such a hypothesis is in agreement with the proteome profile, showing that FDH expression increases under Fe deficiency and decreases under Mo deficiency (Fig. 8). Mo starvation might reduce the pool of transported Fe by affecting, through FDH activity, the Met cycle with a consequent reduction of the biosythesis of nicotianamine. A Mo-dependent regulation of plant FDH cannot be excluded (at any level of control, from transcription to post-translation); this is intriguing as, in contrast to their prokaryotic counterparts, eukaryotic FDH proteins do not require Moco in their active site.

Another open question is the way in which Fe enters mitochondria and whether mitoferrinlike (Mfl) transporters are involved (Fig. 8). In rice (*Oryza sativa*), the mitochondrial Fe transporter MIT1 (mitochondrial iron transporter), a homologue of mitoferrin, has already been identified (Bashir *et al*., 2011). Yet, in Arabidopsis the only published candidate gene *Mitoferrinlike 1* (*AtMfl1*) encodes a protein that is probably involved in the transport of Fe into chloroplasts (Tarantino *et al*., 2011; Haferkamp & Schmitz-Esser, 2012).

Taken together, our results show that the Fe nutritional status dominates over Mo homeostasis and affects Mo uptake, its distribution and its usage in molybdo-enzymes in the form of Moco. One exception to this Fe dominance is the heat-shock protein HSP20 (Csa-6g21760), which changed its expression under combined Mo and Fe starvation only (Table S2) and will therefore be further analysed.

Future elucidation of the most relevant questions raised by the present work will help in understanding the key steps in the control of a plant's nutritional status. In particular, this will include the Mo uptake mechanisms of roots, the role of Mo and in particular of molybdo-enzyme ARC in mitochondria, the impact of FDH activity on the end products of the Met cycle under Mo and Fe deficiency and its putative regulation by Mo, as well as the identification of a mitochondrial Fe transporter, whose activity appears to be dependent on Mo homeostasis.

Acknowledgements

G.V. and I.M. were supported by FIRB 2012 no. RBFR127WJ9, MIUR (Ministero dell'Istruzione, Università e Ricerca). F.B. acknowledges funding through research grants Bi 1075/3-2 and Bi 1075/4-1, DFG (Deutsche Forschungsgemeinschaft). D.D.S., A.M.A. and P.M. were supported by MEF (Ministry of Economy and Finance), Project 'FaReBio di Qualità'. We thank Ralf Bern Klösgen for the donation of the polyclonal antibodies against the translocase of chloroplast envelope Toc33, Mikio Nishimura and Shoij Mano for donations of the polyclonal antibodies against catalase and G. Lucchini for assistance during ICP-MS analyses.

Author contributions

G.V. and I.M. planned the experimental approach. G.V., D.D.S., A.M.A., P.M., S.D., C.G., F.B. and I.M. contributed the data. G.V., F.B., D.D.S. and I.M. discussed the data. I.M. wrote the manuscript, with contributions from G.V. and F.B. to the various drafts.

Supporting Information

Filename	Description
nph14214-sup-0001-SupInfo.pdfPDF document, 536.7 KB	**Fig. S1** Cucumber plants grown for 15 d under single or combined Mo and Fe starvation. **Fig. S2** Cucumber plants grown for 22 d under single or combined Mo and Fe starvation. **Fig. S3** Time course analysis of physiological parameters in cucumber plants grown under single or combined Mo and Fe starvation.

Filename	Description
	Fig. S4 Contents of Mo and Fe in stems of cucumber plants grown under single or combined Mo and Fe starvation. **Fig. S5** Acidification of hydroponic medium by roots of cucumber plants. **Fig. S6** Wilting of cucumber plants after removal from hydroponic medium. **Fig. S7** In gel activities of xanthine dehydrogenase and aldehyde oxidase. **Fig. S8** Western blot analysis of mitochondrial purification. **Fig. S9** Overview of the most relevant ionomes and biochemical changes occurring in roots and leaves of cucumber plants, under Mo or Fe starvation. **Methods S1** Experimental details of the MudPIT proteomic approach.
nph14214-sup-0002-TableS1.xlsapplication/msexcel, 387.5 KB	**Table S1** Proteins identified, in root mitochondria, by MudPIT proteomic analysis
nph14214-sup-0003-TableS2.xlsapplication/msexcel, 78 KB	**Table S2** Proteins differentially expressed in root mitochondria

References

Notes :

- Mo and Fe contents are shown in plants grown for 10 d in control hydroponic medium (+Mo+Fe), in medium devoid of Mo (−Mo), devoid of Fe (−Fe), or devoid of both micronutrients (−Mo−Fe). Each value is the mean ± SE of three independent samples, each containing a single whole plant. Significant differences with respect to controls in the same experimental conditions: **, $P < 0.01$; *, $P < 0.05$, according to Student's *t*-test.
- Proteins were identified by MudPIT (Multidimensional Protein Identification Technology) proteomic analysis of mitochondria purified from roots of cucumber plants grown for 10 d in control medium C (+Mo +Fe), and in medium devoid of molybdenum (Mo) (−Mo), devoid of Fe (−Fe), or devoid of both micronutrients (−Mo−Fe). aSpC, average spectral count; +Mo+Fe (control), $n = 6$; −Mo+Fe, $n = 6$; +Mo−Fe, $n = 8$; −Mo−Fe, $n = 7$. Proteins were selected by linear discriminant analysis (LDA) ($P < 0.05$) and pairwise comparisons between control condition C and a given deficiency condition D were further evaluated using the DAve index (aSpC_C − aSpC_D)/(aSpC_C + aSpC_D)/0.5), where SpC_C and SpC_D are the spectral counts in control (C) and any D condition (−Mo, −Fe, or −Mo−Fe). Fold change was estimated by using the natural logarithm ($\log_e$) of the spectral count ratio aSpC_C/aSpC_D. Positive values of DAve and/or spectral count ratios indicate up-regulation in control C, while negative values of DAve and/or spectral count ratios indicate up-regulation in the deficiency condition D. For a given protein and its pairwise comparison in C with D, the DAve values are conventionally set at either +2 or −2, in case such a protein has been exclusively identified in either C or D, while the

value of the natural logarithm of the spectral count ratio for the same proteins is conventionally set to 100 and −100, respectively. Missing DAve values (and spectral count ratios) indicate that they are not statistically significant.

- Proteins were identified by MudPIT proteomic analysis of mitochondria purified from roots of cucumber plants grown for 10 d in control medium C (+Mo +Fe), and in medium devoid of Mo (−Mo), devoid of iron (Fe) (−Fe), or devoid of both micronutrients (−Mo−Fe). aSpC, average spectral count; +Mo+Fe (control), $n = 6$; −Mo+Fe, $n = 6$; +Mo−Fe, $n = 8$; −Mo−Fe, $n = 7$. Proteins were selected by linear discriminant analysis (LDA) ($P < 0.05$) and pairwise comparisons between control condition C and a given deficiency condition D were further evaluated using the DAve index (aSpC_C − aSpC_D)/(aSpC_C + aSpC_D)/0.5), where SpC_C and SpC_D are the spectral counts in control (C) and in any D condition (−Mo, −Fe, or −Mo−Fe). Fold change was estimated by using the natural logarithm ($\log_e$) of the spectral count ratio aSpC_C/aSpC_D. Positive values of DAve and/or spectral count ratios indicate up-regulation in control C, while negative values of DAve and/or spectral count ratios indicate up-regulation in the deficiency condition D. For a given protein and its pairwise comparison in C with D, the DAve values are conventionally set at either +2 or −2, in case such a protein has been exclusively identified in either C or D, while the value of the natural logarithm of the spectral count ratio for the same proteins is conventionally set to 100 and −100, respectively. Missing DAve values (and spectral count ratios) indicate that they are not statistically significant.
- Proteins were identified by MudPIT proteomic analysis of mitochondria purified from roots of cucumber plants grown for 10 d in control medium C (+Mo +Fe), and in medium devoid of Mo (−Mo), devoid of Fe (−Fe), or devoid of both micronutrients (−Mo−Fe). aSpC, average spectral count; +Mo+Fe (control), $n = 6$; −Mo+Fe, $n = 6$; +Mo−Fe, $n = 8$; −Mo−Fe, $n = 7$. Proteins were selected by linear discriminant analysis (LDA) ($P < 0.05$) and pairwise comparisons between control condition C and a given deficiency condition D were further evaluated using the DAve index (aSpC_C − aSpC_D)/(aSpC_C + aSpC_D)/0.5), where SpC_C and SpC_D are the spectral counts in control (C) and in any D condition (−Mo, −Fe, or −Mo−Fe). Fold change was estimated by using the natural logarithm ($\log_e$) of the spectral count ratio aSpC_C/aSpC_D. Positive values of DAve and/or spectral count ratios indicate up-regulation in control C, while negative values of DAve and/or spectral count ratios indicate up-regulation in the deficiency condition D. For a given protein and its pairwise comparison in C with D, the DAve values are conventionally set at either +2 or −2, in case such a protein has been exclusively identified in either C or D, while the value of the natural logarithm of the spectral count ratio for the same proteins is conventionally set to 100 and −100, respectively. Missing DAve values (and spectral count ratios) indicate that they are not statistically significant.

- Alekseeva AA, Savin SS, Tishkov VI. 2011. NAD^+-dependent formate dehydrogenase from plants. *Acta Naturae* 3: 38–54.
- Anbar AD. 2008. Oceans. Elements and evolution. *Science* 322: 1481–1483.
- Andalus S, Lopez-Millan AF, De las Rivas J, Aro EM, Abadia J, Abadia A. 2006. Proteomic profiles of thylakoid membranes and changes in response to iron deficiency. *Photosynthesis Research* 89: 141–155.

CrossrefCASPubMedWeb of Science®Google ScholarTrova@UniTO

- Araulo WL, Ishizaki K, Nunes-Nesi A, Larson TR, Tohge T, Krahnert I, Witt S, Obata T, Schauer N, Graham IA *et al.* 2010. Identification of the 2-hydroxyglutarate and isovaleryl-CoA dehydrogenase as alternative electron donors linking lysine catabolism to the electron transport chain of Arabidopsis mitochondria. *Plant Cell* 22: 1549–1563.

- Balk J, Leaver CJ. 2001. The PET1-CMS mitochondrial mutation in sunflower is associated with premature programmed cell death and cytochrome c release. *Plant Cell* 13: 1803–1818.
- Balk J, Schaedler TA. 2014. Iron cofactor assembly in plants. *Annual Review of Plant Physiology* 65: 125–153.
- Bashir K, Ishimaru Y, Shimo H, Nagasaka S, Fujimoto M, Takanashi H, Tsutsumi N, An G, Nakanishi H, Nishizawa NK. 2011. The rice mitochondrial iron transporter is essential for plant growth. *Nature Communications* 2: 322.
- Baxter I. 2009. Ionomics: studying the social network of mineral nutrients. *Current Opinion in Plant Biology* 12: 381–386.
- Baxter I, Muthukumar B, Park HC, Buchner P, Lahner B, Danku J, Zhao K, Lee J, Hawkesford MJ, Guerinot ML *et al*. 2008b. Variation in molybdenum content across broadly distributed populations of *Arabidopsis thaliana* is controlled by a mitochondrial Molybdenum Transporter (MOT1). *PLoS Genetics* 4: e1000004.
- Baxter I, Vitek O, Lahner B, Muthukumar B, Borghi M, Morrissey J, Guerinot ML, Salt DE. 2008a. The leaf ionome as a multivariable system to detect a plant's physiological status. *Proceedings of the National Academy of Sciences, USA* 105: 12081–12086.
- Bittner F. 2014. Molybdenum metabolism in plants and crosstalks to iron. *Frontiers in Plant Science* 5: 28.
- Bittner F, Mendel RR. 2010. Cell biology of molybdenum. In: Hell R, Mendel RR, eds. Cell biology of metals and nutrients. Plant Cell Monogr, 17. Berlin, Heidelberg: Springer-Verlag, 119–143.
- Borlotti A, Vigani G, Zocchi G. 2012. Iron deficiency affects nitrogen metabolism in cucumber (*Cucumis sativus* L.) plants. *BMC Plant Biology* 12: 189.
- Briat JF, Dubos C, Gaymard F. 2015a. Iron nutrition, biomass production and plant product quality. *Trends in Plant Science* 20: 33–40.
- Briat JF, Rouached H, Tissot N, Gaymard F, Dubos C. 2015b. Integration of P, S, Fe and Zn nutrition signals in *Arabidopsis thaliana*: potential involvement of PHOSPHATE STARVATION RESPONSE 1 (PHR1). *Frontiers in Plant Science* 6: 290.
- Brychkova G, Alikulov Z, Fluhr R, Sagi M. 2008. A critical role for ureides in dark and senescence-induced purine remobilization is unmasked in the Atxdh1 *Arabidopsis* mutant. *Plant Journal* 54: 496–509.
- Carr S, Aebersold R, Baldwin M, Burlingame A, Clauser K, Nesvizhskii A. 2004. The need for guidelines in publication of peptide and protein identification data: working group on publication guidelines for peptide and protein identification data. *Molecular & Cellular Proteomics: MCP* 3: 531–533.
- Carvalho PC, Fischer JSG, Chen EI, Yates JR 3rd, Barbosa VC. 2008. PatternLab for proteomics: a tool for differential shotgun proteomics. *BMC Bioinformatics* 9: 316.
- Chamizo-Ampudia A, Galvan A, Fernandez E, Llamas A. 2011. The *Chlamydomonas reinhardtii* molybdenum cofactor enzyme crARC has a Zn-dependent activity and protein partners similar to those of its human homologue. *Eukaryotic Cell* 10: 1270–1282.
- Ciaffi M, Paolacci AR, Celletti S, Catarcione G, Kopriva S, Astolfi S. 2013. Transcriptional and physiological changes in the S assimilation pathway due to single or combined S and Fe deprivation in durum wheat (*Triticum durum* L.) seedlings. *Journal of Experimental Botany* 64: 1663–1675.
- Colangelo EP, Guerinot ML. 2004. The essential basic helix-loop-helix protein FIT1 is required for the iron deficiency response. *Plant Cell* 16: 3400–3412.
- Colinas M, Fitzpatrick TB. 2015. Natures balancing act: examining biosynthesis de novo, recycling and processing damaged vitamin B metabolytes. *Current Opinion in Plant Biology* 25: 98–106.
- Cosentino C, Di Silvestre D, Fischer-Schliebs E, Homann U, De Palma A, Comunian C, Mauri PL, Thiel G. 2013. Proteomic analysis of *Mesembryanthemum crystallinum* leaf microsomal fractions finds an imbalance in V-ATPase stoichiometry during the salt-induced transition from C3 to CAM. *Biochemical Journal*. 450: 407–415.
- Delahunty CM, Yates JR III. 2007. MudPIT: multidimensional protein identification technology. *BioTechniques* 43: 563, 565, 567
- Dell'Orto M, Pirovano L, Villalba JM, Gonzalez-Reyes JA, Zocchi G. 2002. Localization of the plasma membrane H^+-ATPase in Fe-deficient cucumber roots by immunodetection.
- Donnini S, Prinsi B, Negri AS, Vigani G, Espen L, Zocchi G. 2010. Proteomic characterization of iron deficiency responses in *Cucumis sativus* L. roots. *BMC Plant Biology* 10: 268.

- Ducret A, Van Oostveen I, Eng JK, Yates J III, Aebersold R. 1998. High throughput protein characterization by automated reverse-phase chromatography/electrospray tandem mass spectrometry. *Protein Science* 7: 706–719.
- Fitzpatrick KL, Tyerman SD, Kaiser BN. 2008. Molybdate transport through the plant sulfate transporter SHST1. *FEBS Letters* 582: 1508–1513.
- Forieri I, Wirtz M, Hell R. 2013. Toward new perspectives on the interaction of iron and sulfur metabolism. *Frontiers in Plant Science* 4: 357.
- Gasber A, Klaumann S, Trentmann O, Trampczynska A, Clemens S, Schneider S, Sauer N, Feifer I, Bittner F, Mendel RR *et al*. 2011. Identification of an *Arabidopsis* solute carrier critical for intracellular transport and inter-organ allocation of molybdate. *Plant Biology* 13: 710–718.
- Gerdes S, Lerma-Ortiz C, Frelin O, Seaver SMD, Henry CS, de Crécy-Lagard V, Hanson AD. 2012. Plant B vitamin pathways and their compartmentation: a guide for the perplexed. *Journal of Experimental Botany* 63: 695–709.
- Grimm S. 2012. The ER-mitochondria interface: the social network of cell death. *Biochimica et Biophysica Acta* 1823: 327–334.
- Gruenewald S, Wahl B, Bittner F, Hungeling H, Kanzow S, Kotthaus J, Schwering U, Mendel RR, Clement B. 2008. The fourth molybdenum containing enzyme mARC: cloning and involvement in the activation of N-hydroxylated prodrugs. *Journal of Medicinal Chemistry* 51: 8173–8177.
- Haferkamp I, Schmitz-Esser S. 2012. The plant mitochondrial carrier family: functional and evolutionary aspects. *Frontiers in Plant Science* 3: 2.
- Havelund JF, Thelen JJ, Moller IM. 2013. Biochemistry, proteomics and phosphoproteomics of plant mitochondria from non-photosynthetic cells. *Frontiers in Plant Science* 4: 51.
- Herbik A, Ciritch A, Horstmann C, Becker R, Balzer HJ, Baumlein H, Udo WS. 1996. Iron and copper nutrition-dependent changes in protein expression in a tomato wild type and the nicotianamine-free mutant *chloronerva*. *Plant Physiology* 11: 533–540.
- Hesberg C, Haensch R, Mendel RR, Bittner F. 2004. Tandem orientation of duplicated xanthine dehydrogenase genes from *Arabidopsis thaliana*: differential gene expression and enzyme activities. *Journal of Biological Chemistry* 279: 13547–13554.
- Hilario M, Kalousis A. 2008. Approaches to dimensionality reduction in proteomic biomarker studies. *Briefings in Bioinformatics* 9: 102–118.
- Ide Y, Kusano M, Oikawa A, Fukushima A, Tomatsu H, Saito K, Hirai MY, Fujiwara T. 2011. Effects of molybdenum deficiency and defects in molybdate transporter MOT1 on transcript accumulation and nitrogen/sulphur metabolism in *Arabidopsis thaliana*. *Journal of Experimental Botany* 62: 1483–1497.
- Itai RN, Ogo Y, Kobayashi T, Nakanishi H, Nishizawa NK. 2013. Rice genes involved in phytosiderophore biosynthesis are synchronously regulated during the early stages of iron deficiency in roots. *Rice* 6: 16.
- Ivanov R, Brumbarova T, Bauer P. 2012. Fitting into the harsh reality: regulation of iron deficiency responses in dicotyledonous plants. *Molecular Plant* 5: 27–42.
- Jain AK, Murty MN, Flynn PJ. 1999. Data clustering: a review. *ACM Computing Surveys* 31: 264–323.
- Jeong J, Guerinot ML. 2009. Homing in on iron homeostasis in plants. *Trends in Plant Science* 14: 280–285.
- Kaiser BN, Gridley KL, Brady JN, Phillips T, Tyerman SD. 2005. The role of molybdenum in agricultural plant production. *Annals of Botany* 96: 745–754.
- Kobayashi T, Nishizawa NK. 2012. Iron uptake, translocation and regulation in higher plants. *Annual Review of Plant Biology* 63: 131–152.
- Kobayashi T, Nishizawa NK. 2014. Iron sensors and signals in response to iron deficiency. *Plant Science* 224: 36–43.
- Kobayashi T, Suzuki M, Inoue H, Nakanishi Itai R, Takahashi M, Nakanishi H, Mori S, Nishizawa NK. 2005. Expression of iron-acquisition-related genes in iron-deficient rice is co-ordinately induced by partially conserved iron-deficiency-responsive elements. *Journal of Experimental Botany* 56: 1305–1316.
- Koshiba T, Saito E, Ono N, Yamamoto N, Sato M. 1996. Purification and properties of flavin- and molybdenum-containing aldehyde oxidase from coleoptiles of maize. *Plant Physiology* 110: 781–789.
- Kotthaus J, Wahl B, Havemeyer A, Kotthaus J, Schade D, Garbe-Schoenberg D, Mendel R, Bittner F, Clement C. 2011. Reduction of Nω-hydroxy-L-arginine by the mitochondrial amidoxime reducing component (mARC). *Biochemical Journal* 433: 383–391.

- Kumar R, Phan Tran LS, Neelakandar AK, Nguyen HT. 2012. Higher plant cytochrome b5 polypetides modulate fatty acid desaturation. *PLoS ONE* 7: e31370.
- Laganowsky A, Gomez SM, Whitelegge JP, Nishio JN. 2009. Hydroponics on a chip. Analysis of the Fe deficient *Arabidopsis* thylakoid membrane proteome. *Journal of Proteomics* 72: 397–415.
- Lan P, Li W, Wen TN, Shiau JY, Wu YC, Lin W, Schmidt W. 2011. iTRAQ protein profile analysis of *Arabidopsis* roots reveals new aspects critical for Fe homeostasis. *Plant Physiology* 155: 821–834.
- Li J, Hao ST, Wang XJ, Ling HQ. 2008. Proteomic response to iron deficiency in tomato root. *Proteomics* 8: 2299–2311.
- Li Y, Wang N, Zhao F, Song X, Yin Z, Huang R, Zhang C. 2014. Changes in the transcriptomic profiles of maize roots in response to iron-deficiency stress. *Plant Molecular Biology* 85: 349–363.
- Lima MRM, Diaz SO, Lamego I, Grusak MA, Vasconcelos MV, Gil AM. 2014. Nuclear magnetic resonance metabolomics of iron deficiency in soybean leaves. *Journal of Proteome Research* 13: 3075–3087.
- Lingam S, Mohrbacher J, Brumbarova T, Potuschak T, Fink-Straube C, Blondet E, Genschik P, Bauer P. 2011. Interaction between the bHLH transcription factor FIT and ETHYLENE INSENSITIVE3/ETHYLENE INSENSITIVE3-LIKE1 reveals molecular linkage between the regulation of iron acquisition and ethylene signaling in *Arabidopsis*. *Plant Cell* 23: 1815–1829.
- Llamas A, Tejada-Jimenez M, Fernandez E, Galvan A. 2011. Molybdenum metabolism in the alga *Chlamydomonas* stands at the cross road of those in *Arabidopsis* and humans. *Metallomics* 3: 578–590.
- Lopez-Millan AF, Grusak MA, Abadia A, Abadia J. 2013. Iron deficiency in plants: an insight from proteomic approaches. *Frontiers in Plant Science* 4: 254.
- Mauri P, Dehò G. 2008. A proteomic approach to the analysis of RNA degradosome composition in *Escherichia coli*. *Methods in Enzymology* 447: 99–117.
- Mauri P, Scarpa A, Nascimbeni AC, Benazzi L, Parmagnani E, Mafficini A, Della Peruta M, Bassi C, Miyazaki K, Sorio C. 2005. Identification of proteins released by pancreatic cancer cells by multidimensional protein identification technology: a strategy for identification of novel cancer markers. *FASEB Journal* 19: 1125–1127.
- Meiser J, Lingam S, Bauer P. 2011. Posttranslational regulation of the iron deficiency basic helix-loop-helix transcription factor FIT is affected by iron and nitric oxide. *Plant Physiology* 157: 2154–2166.
- Millar AH, Liddell A, Leaver CL. 2007. Isolation and subfractionation of mitochondria from plants. *Methods in Cell Biology* 80: 65–90.
- Miyazaki JH, Yang SF. 1987. The methionine salvage pathway in relation to ethylene and polyamine biosynthesis. *Physiologia Plantarum* 69: 366–370.
- Moran Lauter AN, Peiffer GA, Yin T, Whitham SA, Cook D, Shoemaker RC, Graham MA. 2014. Identification of candidate genes involved in early iron deficiency chlorosis signaling in soybean (*Glycine max*) roots and leaves. *BMC Genomics* 15: 702.
- Muller-Taubenberger A, Lupas AN, Li H, Ecke M, Simmeth E, Gerisch G. 2001. Calreticulin and calnexin in the endoplasmic reticulum are important for phagocytosis. *EMBO Journal* 20: 6772–6782.
- Murgia I, Vigani G. 2015. Analysis of *Arabidopsis thaliana atfer4-1*, *atfh* and *atfer4-1/atfh* mutants uncovers frataxin and ferritin contributions to leaf ionome homeostasis. *Plant Physiology and Biochemistry* 94: 65–72.
- Nakagawa A, Sakamoto S, Takahashi M, Morikawa H, Sakamoto A. 2007. The RNAi-mediated silencing of xanthine dehydrogenase impairs growth and fertility and accelerates leaf senescence in transgenic *Arabidopsis* plants. *Plant and Cell Physiology* 48: 1484–1495.
- Nziengui H, Bouhidel K, Der C, Marty F, Schoefs BI. 2007. Reticulon-like proteins in *Arabidopsis thaliana*: structural organization and ER localization. *FEBS Letters* 581: 3356–3362.
- Ott G, Havemeyer A, Clement B. 2015. The mammalian molybdenum enzymes of mARC. *JBIC Journal of Biological Inorganic Chemistry* 20: 265–275.
- Palmer C, Guerinot ML. 2009. A question of balance: facing the challenges of Cu, Fe and Zn homeostasis. *Nature Chemical Biology* 5: 333–340.
- Paolacci AR, Celletti S, Catarcione G, Hawkesford MJ, Astolfi S, Ciaffi M. 2014. Iron deprivation results in a rapid but not sustained increase of the expression of genes involved in iron metabolism and sulfate uptake in tomato (*Solanum lycopersicum* L.) seedlings. *Journal of Integrative Plant Biology* 56: 88–100.
- Peng C, Uygun S, Shiu SH, Last RL. 2015. The impact of the branched-chain ketoacid dehydrogenase complex on amino acid homeostasis in Arabidopsis. *Plant Physiology* 169: 1807–1820.

- Ravet K, Pilon M. 2013. Copper and iron homeostasis in plants: the challenges of oxidative stress. *Antioxidants & Redox Signaling* 19: 919–932.
- Regonesi ME, Del Favero M, Basilico F, Briani F, Benazzi L, Tortora P, Mauri P, Dehò G. 2006. Analysis of the *Escherichia coli* RNA degradosome composition by a proteomic approach. *Biochimie* 88: 151–161.
- Rellán-Álvarez R, Andaluz S, Rodríguez-Celma J, Wohlgemuth G, Zocchi G, Álvarez- Fernández A, Fiehn O, López-Millán AF, Abadía J. 2010. Changes in the proteomic and metabolic profiles of *Beta vulgaris* root tips in response to iron deficiency and resupply. *BMC Plant Biology* 10: 120–134.
- Rellán-Álvarez R, El-Jendoubi H, Wohlgemuth G, Abadía A, Fiehn O, Abadía J, Álvarez-Fernández A. 2011. Metabolite profile changes in xylem sap and leaf extracts of strategy I plants in response to iron deficiency and resupply. *Frontiers in Plant Science* 2: 66.
- Ro DK, Mah N, Ellis BE, Douglas CJ. 2001. Functional characterization and subcellular localization of poplar (*Populus trichocarpa* × *Populus deltoides*) cinnamate 4-hydroxylase. *Plant Physiology* 126: 317–329.
- Rödiger A, Baudisch B, Klösgen EB. 2010. Simultaneous isolation of intact mitochondria and chloroplasts from a single pulping of plant tissue. *Journal of Plant Physiology* 167: 620–624.
- Rodriguez-Celma J, Pan IC, Li W, Lan P, Buckhout TJ, Schmidt W. 2013. The transcriptional response of *Arabidopsis* leaves to Fe deficiency. *Frontiers in Plant Science* 4: 276.
- Santi S, Schmidt W. 2009. Dissecting iron deficiency-induced proton extrusion in *Arabidopsis* roots. *New Phytologist* 183: 1072–1084.
- Schaedler TA, Thornton JD, Kruse I, Schwarzländer M, Meyer AJ, van Veen HW, Balk J. 2014. A conserved mitochondrial ATP-binding cassette transporter exports gluthatione polysulfide for cytosolic metal cofactor assembly. *Journal of Biological Chemistry* 289: 23264–23274.
- Schinmachi F, Buchner P, Stroud J, Parmar S, Zhao FJ, McGrath SP, Hawkesford MJ. 2010. Influence of sulfur deficiency on the expression of specific sulfate transporters and the distribution of sulfur, selenium and molybdenum in wheat. *Plant Physiology* 153: 327–336.
- Schmidt H, Günther C, Weber M, Spörlein C, Loscher S, Böttcher C, Schobert R, Clemens S. 2014. Metabolome analysis of *Arabidopsis thaliana* roots identifies a key metabolic pathway for iron acquisition. *PLoS ONE* 9: e102444.
- Schuler M, Keller A, Backes C, Philippar K, Lenhof HP, Bauer P. 2011. Transcriptome analysis by GeneTrail revealed regulation of functional categories in response to alterations of iron homeostasis in *Arabidopsis thaliana*. *BMC Plant Biology* 11: 87.
- Shinmachi F, Buchner P, Stroud JL, Parmar S, Zhao FJ, McGrath SP, Hawkesford MJ. 2010. Influence of sulfur deficiency on the expression of specific sulfate transporters and the distribution of sulfur, selenium, and molybdenum in wheat. *Plant Physiology* 153: 327–336.
- Silvestro D, Andersen TG, Schaller H, Jensen PE. 2013. Plant sterol metabolism. Δ^{7} –sterol-C5-desaturase (STE1/DWARF7), $\Delta^{5,7}$ –sterol- Δ^{7} -reductase (DWARF5) and Δ^{24} -sterol- Δ^{24}- reductase (DIMINUTO/DWARF1) show multiple subcellular localization in *Arabidopsis thaliana* (Heynh) L. *PLoS ONE* 8: e56429.
- Sudre D, Gutierrez-Carbonell E, Lattanzio G, Rellan-Alvarez R, Gaymard F, Wohlgemuth G, Fiehn O, Alvarez-Fernandez A, Zamarreño AG, Bacaicoa E *et al*. 2013. Iron-dependent modifications of the flower transcriptome, proteome, metabolome, and hormonal content in an *Arabidopsis* ferritin mutant. *Journal of Experimental Botany* 64: 2665–2688.
- Suzuki K, Itai R, Suzuki K, Nakanishi H, Nishizawa NK, Yoshimura E, Mori S. 1998. Formate dehydrogenase, an enzyme of anaerobic metabolism, is induced by iron deficiency in barley roots. *Plant Physiology* 116: 725–732.
- Tan YF, O'Toole N, Taylor NL, Millar AH. 2010. Divalent metal ions in plant mitochondria and their role in interaction with proteins and oxidative stress-induced damage to respiratory function. *Plant Physiology* 152: 747–761.
- Tarantino D, Casagrande F, Soave C, Murgia I. 2010. Knocking out of the mitochondrial AtFer4 ferritin does not alter response of *Arabidopsis* plants to abiotic stresses. *Journal of Plant Physiology* 167: 453–460.
- Tarantino D, Morandini P, Ramirez L, Soave C, Murgia I. 2011. Identification of an Arabidopsis mitoferrinlike carrier protein involved in Fe metabolism. *Plant Physiology and Biochemistry* 49: 520–529.

- Tarantino D, Vannini C, Bracale M, Campa M, Soave C, Murgia I. 2005. Antisense reduction of thylakoidal ascorbate peroxidase in *Arabidopsis* enhances Paraquat-induced photooxidative stress and nitric oxide-induced cell death. *Planta* 221: 757–765.
- Teschner J, Lachmann N, Schulze J, Geisler M, Selbach K, Santamaria-Araujo J, Balk J, Mendel RR, Bittner F. 2010. A novel role for *Arabidopsis* mitochondrial ABC transporter ATM3 in molybdenum cofactor biosynthesis. *Plant Cell* 22: 468–480.
- Timperio AM, D'Amici GM, Barta C, Loreto F, Zolla L. 2007. Proteomics, pigment composition and organization of thylakoid membranes in iron-deficient spinach leaves. *Journal of Experimental Botany* 58: 3695–3710.
- Tomatsu H, Takano J, Takahashi H, Watanabe-Takahashi A, Shibagaki N, Fujiwara T. 2007. An *Arabidopsis thaliana* high-affinity molybdate transporter required for efficient uptake of molybdate from soil. *Proceedings of the National Academy of Sciences, USA* 104: 18807–18812.
- Vigani G. 2012. Discovering the role of mitochondria in the iron deficiency-induced metabolic responses of plants. *Journal of Plant Physiology* 169: 1–11.
- Vigani G, Bashir K, Ishimaru Y, Lehmann M, Casiraghi FM, Nakanishi H, Seki M, Geigenberger P, Zocchi G, Nishizawa NK. 2016. Knocking down mitochondrial iron transporter (MIT) reprograms primary and secondary metabolism in rice plants. *Journal of Experimental Botany* 67: 1357–1368.
- Vigani G, Maffi D, Zocchi G. 2009. Iron availability affects the function of mitochondria in cucumber roots. *New Phytologist* 182: 127–136.
- Vigani G, Zocchi G. 2010. Effect of Fe deficiency on mitochondrial alternative NAD(P)H dehydrogenases in cucumber roots. *Journal of Plant Physiology* 167: 666–669.
- Vigani G, Morandini P, Murgia I. 2013a. Searching iron sensors in plants by exploring the link among 2′-OG-dependent dioxygenases, the iron deficiency response and metabolic adjustments occurring under iron deficiency. *Frontiers in Plant Science* 4: 169.
- Vigani G, Tarantino D, Murgia I. 2013b. Mitochondrial ferritin is a functional iron storage protein in cucumber (*Cucumis sativus*) roots. *Frontiers in Plant Science* 4: 316.
- Vigani G, Zocchi G, Bashir K, Philippar K, Briat JF. 2013c. Signal for chloroplast and mitochondria for iron homeostasis regulation. *Trends in Plant Science* 18: 305–311.
- Wang G, Wu WW, Zhang Z, Masilamani S, Shen RF. 2009. Decoy methods for assessing false positives and false discovery rates in shotgun proteomics. *Analytical Chemistry* 81: 146–159.
- Witte CP, Igeño MI, Mendel R, Schwarz G, Fernandez E. 1998. The *Chlamydomonas reinhardtii* MoCo carrier protein is multimeric and stabilizes molybdopterin cofactor in a molybdate charged form. *FEBS Letters* 431: 205–209.
- Yamaguchi J, Nishimura M. 1984. Purification of glyoxysomal catalase and immunochemical comparison of glyoxysomal and leaf peroxisomal catalase in germinating pumpkin cotyledons. *Plant Physiology* 74: 261–267.
- Yang J, Giles LJ, Ruppelt C, Mendel RR, Bittner F, Kirk ML. 2015. Oxyl and hydroxyl radical transfer in mitochondrial amidoxime reducing component-catalyzed nitrite reduction. *Journal of the American Chemical Society* 137: 5276–5279.
- Yokoyama K, Leimkühler S. 2015. The role of FeS clusters for molybdenum cofactor biosynthesis and molybdoenzymes in bacteria. *Biochimica et Biophysica Acta* 1853: 1335–1349.
- Zhao Y, Karypis G. 2005. Data clustering in life sciences. *Molecular Biotechnology* 31: 55–80.
- Zuchi S, Watanabe M, Hubberten HM, Bromke M, Osorio S, Fernie AR, Celletti S, Paolacci AR, Catarcione G, Ciaffi M *et al*. 2015. The interplay between sulfur and iron nutrition in tomato. *Plant Physiology* 169: 2624–2639.